Workshop on
Gauge Theory and String Theory

ETH Zürich, Switzerland

2 - 4 July 2008

Different aspects of the theory and phenomenology of the BFKL formalism

1. QCD at high energies
2. Linear evolution
3. Vector meson production
4. Jet production: LHC & HERA
5. Unitarity in DIS
6. Open questions

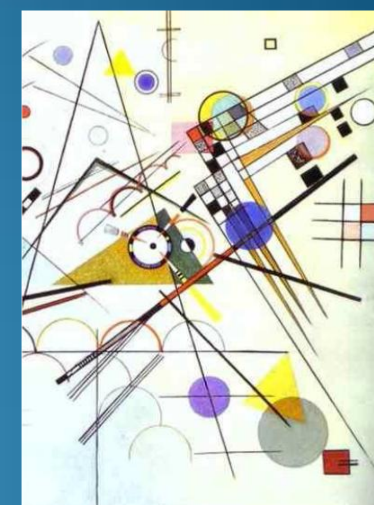

Agustín Sabio Vera

CERN

1. QCD at high energies

Some good books:

"QCD and the Pomeron"
Forshaw, Ross

"Pomeron physics and QCD"
Donnachie, Dosh, Landshoff, Nachtmann

"High energy particle diffraction"
Barone, Predazzi

High energy limit of scattering amplitudes in QCD:

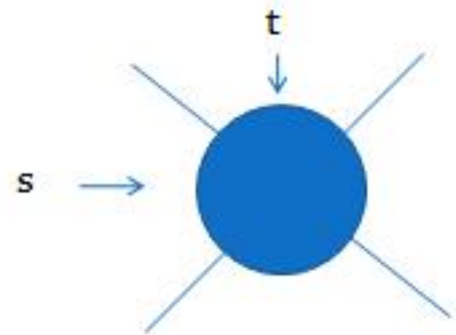

$$s \gg |t|,\ Q^2 \gg \Lambda^2_{QCD}$$

$$\alpha_s(Q^2) \ll 1$$

Large logarithms in s compensate small coupling and a full resummation is needed:

$$\text{BFKL} \sim \sum_{n=1}^{\infty} (\alpha_s \ln s)^n$$

In multi-Regge kinematics:

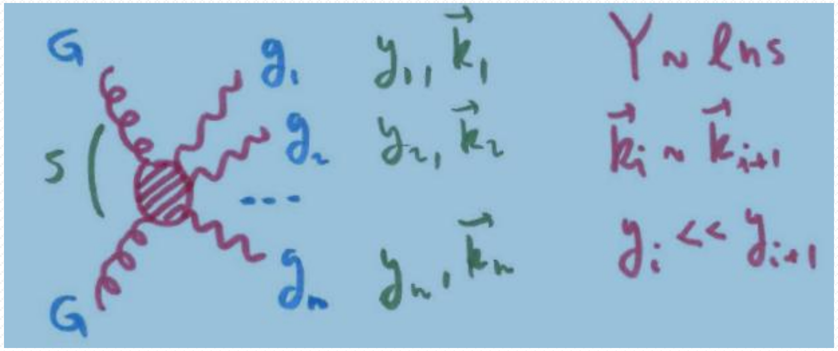

$$\bar{\alpha}_s^n \int_0^Y dy_1 \int_0^{y_1} dy_2 \cdots \int_0^{y_{n-1}} dy_n \sim \frac{(\alpha_s Y)^n}{n!}$$

In this limit new effective degrees of freedom appear

VIRTUAL contributions Reggeize t-channel gluons

REAL emissions create a gauge invariant effective vertex

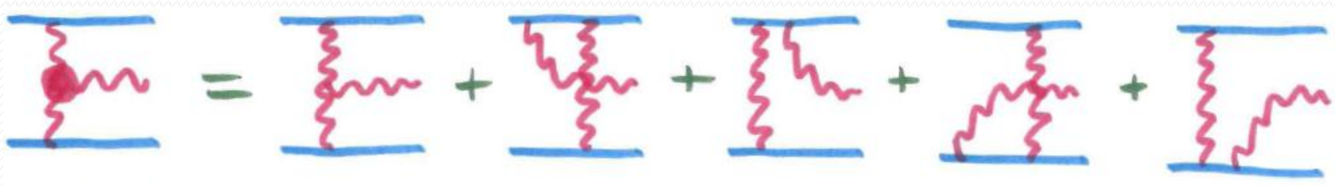

2 to 2+n soft gluon amplitudes have ladder structure

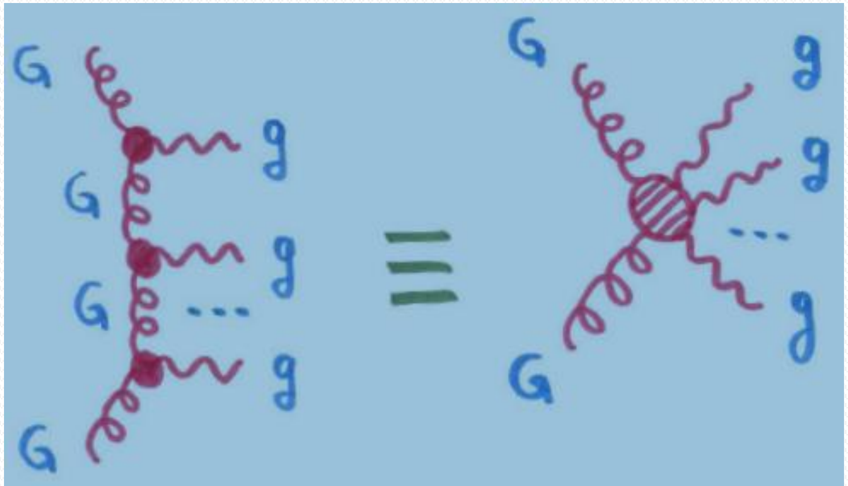

Multijet cross sections:

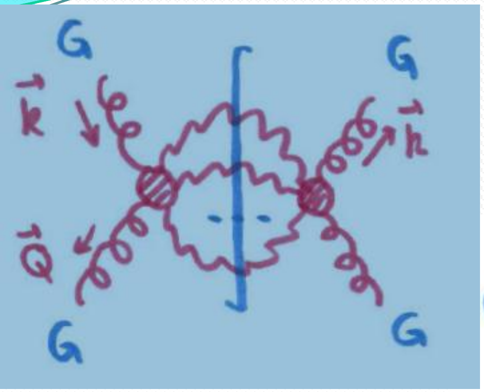

$$f(\vec{k},\vec{Q},Y) \sim \sum_{n=-\infty}^{\infty} \int \frac{d\omega}{2\pi i} e^{\omega Y} \int \frac{d\gamma}{2\pi i} \left(\frac{\vec{k}^2}{\vec{Q}^2}\right)^{\gamma} \frac{e^{in\theta}}{\omega - \bar{\alpha}_s \chi_n(\gamma)}$$

$$\chi_n(\gamma) = 2\psi(1) - \psi\left(\gamma + \frac{|n|}{2}\right) - \psi\left(1-\gamma+\frac{|n|}{2}\right)$$

↳ conformal spins

Diffractive events:

Hard Pomeron = bound state of 2 Reggeized gluons.

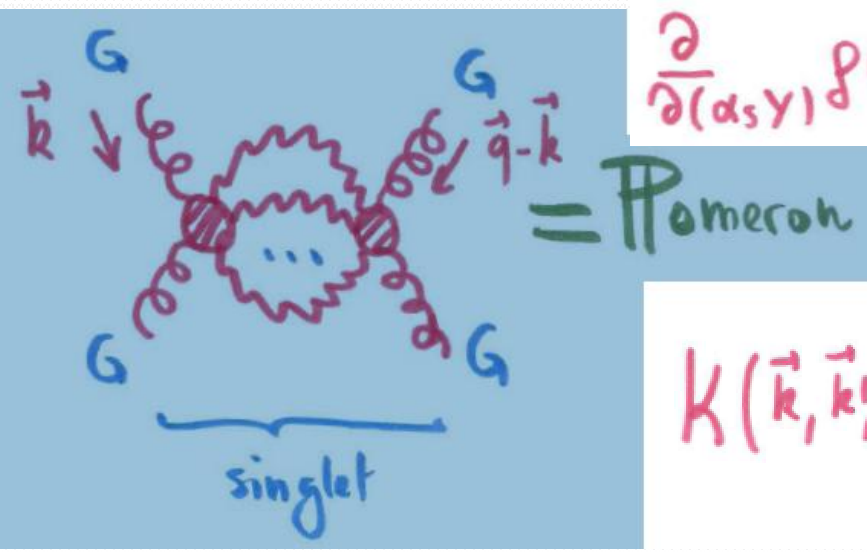

$$\frac{\partial}{\partial(\alpha_s Y)} f(\vec{k},\vec{q},Y) = \int d\vec{k}' \, K(\vec{k},\vec{k}',\vec{q}) \, f(\vec{k}',\vec{q},Y)$$

$$q = q_x + i\, q_y \qquad q^* = q_x - i\, q_y$$

$$K(\vec{k},\vec{k}',\vec{q}) \qquad z_i \rightarrow z_i' = \frac{a z_i + b}{c z_i + d}$$

Phenomenology of multi-Regge kinematics:

Uncut diagram

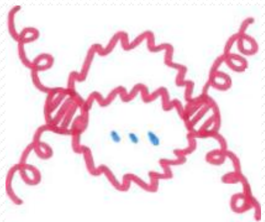

describes DIFFRACTIVE events with rapidity gaps

Lepton-lepton | Hadron-hadron | Lepton-hadron

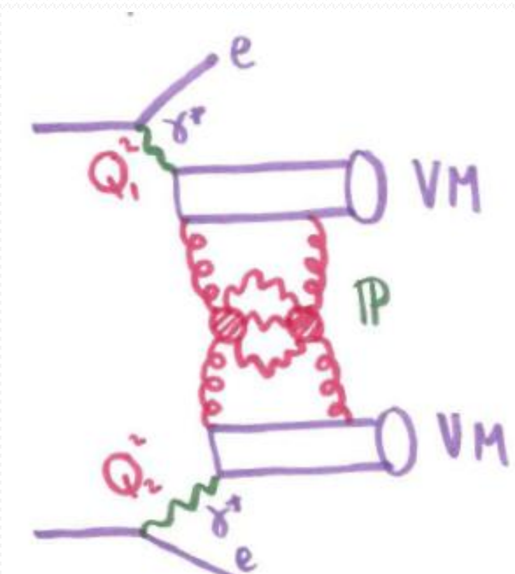

Production of light vector mesons

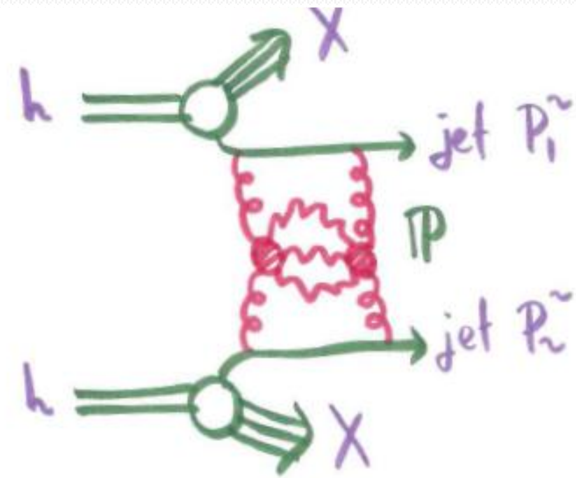

Mueller-Tang jets

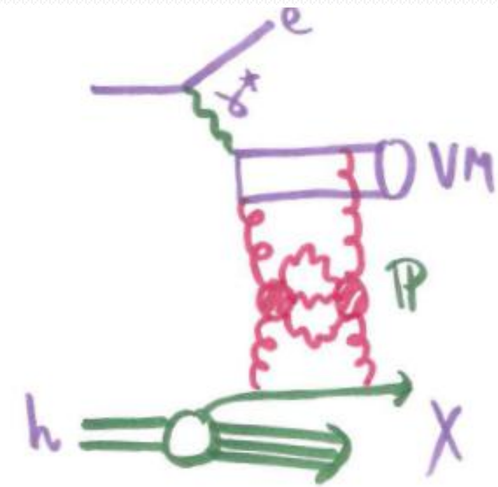

Vector meson production in DIS

Cut diagram

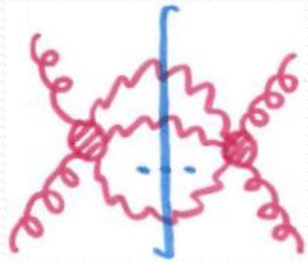

describes high multiplicity events

Multi-jet events with 2 large and similar hard scales:

Lepton-lepton

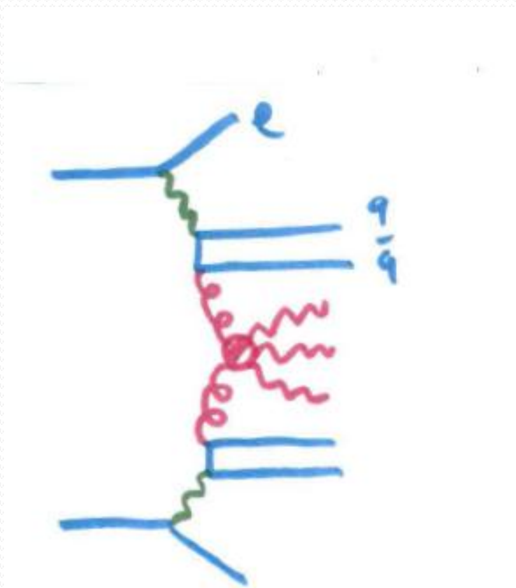

Total cross section for two virtual photons

Hadron-hadron

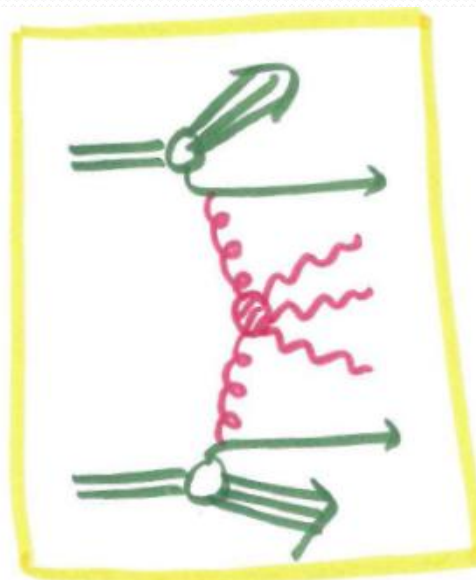

Mueller-Navelet jets

Lepton-hadron

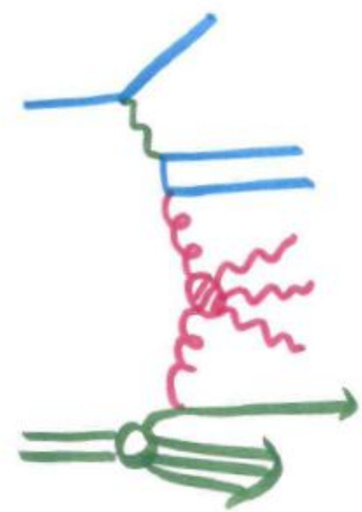

Forward jets in DIS

2. Linear evolution

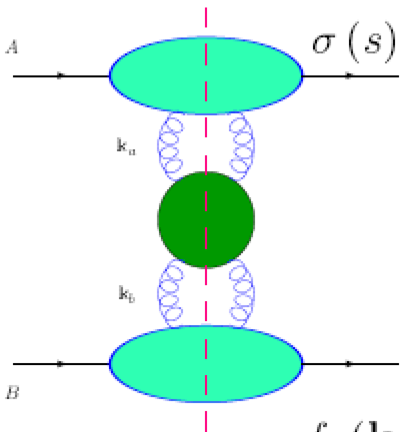

$$\sigma(s) = \int \frac{d^2\mathbf{k}_a}{\mathbf{k}_a^2} \int \frac{d^2\mathbf{k}_b}{\mathbf{k}_b^2} \Phi_A(\mathbf{k}_a)\, \Phi_B(\mathbf{k}_b)\, f\left(\mathbf{k}_a, \mathbf{k}_b, \mathrm{Y} = \ln \frac{s}{s_0}\right)$$

$$f(\mathbf{k}_a, \mathbf{k}_b, \mathrm{Y}) = \frac{1}{2\pi i} \int_{a-i\infty}^{a+i\infty} d\omega\; e^{\omega \mathrm{Y}} f_\omega(\mathbf{k}_a, \mathbf{k}_b)$$

$$\omega f_\omega(\mathbf{k}_a, \mathbf{k}_b) = \delta^{(2)}(\mathbf{k}_a - \mathbf{k}_b) + \int d^2\mathbf{k}\; \mathcal{K}(\mathbf{k}_a, \mathbf{k}) f_\omega(\mathbf{k}, \mathbf{k}_b)$$

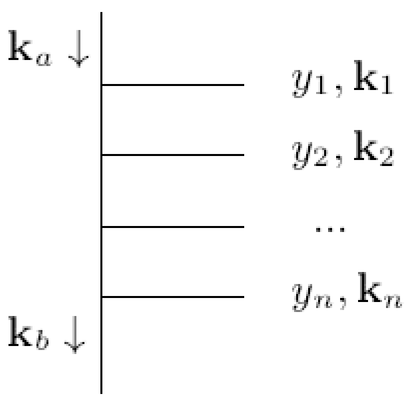

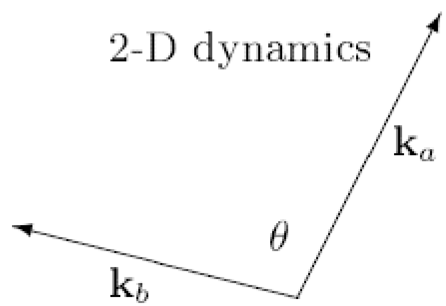

Drawbacks of LL approximation:

- Intercept is too large when compared with experiment
- α_s is a fixed constant
- s_0 is arbitrary
- Diffusion of internal momenta into the infrared region.

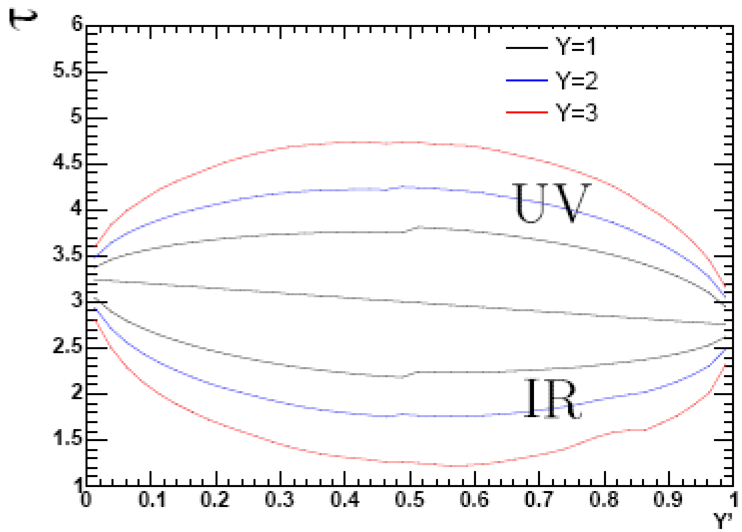

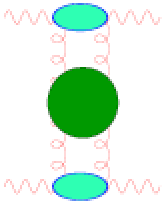

To run the coupling & fix the energy scale in Y:

quasi–multiRegge kinematics

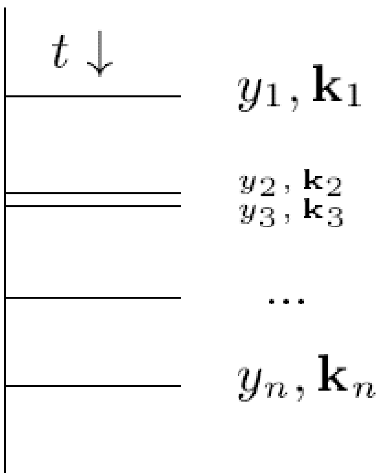

$\mathbf{k}_i \sim \mathbf{k}_{i+1}$

$y_i << y_{i+1}$

$y_2 \sim y_3$

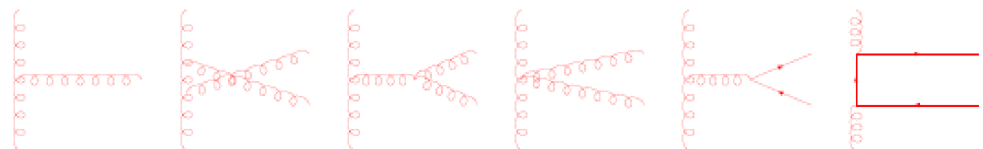

NLL BFKL Equation: $(\alpha_S \mathrm{Y})^n + \alpha_S(\alpha_S \mathrm{Y})^n$

$$\sigma(s) = \int \frac{d^2\mathbf{k}_a}{\mathbf{k}_a^2} \int \frac{d^2\mathbf{k}_b}{\mathbf{k}_b^2} \Phi_A(\mathbf{k}_a)\, \Phi_B(\mathbf{k}_b) f(\mathbf{k}_a, \mathbf{k}_b, \mathrm{Y})$$

$$\omega f_\omega(\mathbf{k}_a, \mathbf{k}_b) = \delta^{(2+2\epsilon)}(\mathbf{k}_a - \mathbf{k}_b) + \int d^{2+2\epsilon}\mathbf{k}\, \mathcal{K}(\mathbf{k}_a, \mathbf{k})\, f_\omega(\mathbf{k}, \mathbf{k}_b)$$

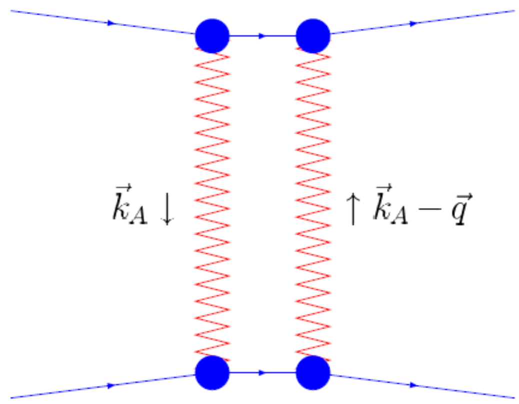

$$\omega_0(t) \;=\; -\frac{\bar{\alpha}_s\, \vec{q}^{\,2}}{4\pi} \int \frac{d^2\vec{k}}{\vec{k}^2(\vec{q}-\vec{k})^2} \;\simeq\; -\frac{\bar{\alpha}_s}{2} \log\left(\frac{\vec{q}^{\,2}}{\mu^2}\right)$$

μ is an infrared regulator

$$\varphi\left(\vec{k}_A, \vec{k}_B, \vec{q}, \mathrm{Y}\right) \;=\; e^{\omega_0\left(-\vec{k}_A^2\right)\mathrm{Y}}\, e^{\omega_0\left(-\left(\vec{k}_B-\vec{q}\right)^2\right)\mathrm{Y}}\, \delta^{(2)}\left(\vec{k}_A - \vec{k}_B\right)$$

$$\varphi\left(\vec{k}_A, \vec{k}_B, \vec{q}, \mathrm{Y}=0\right) \;=\; \delta^{(2)}\left(\vec{k}_A - \vec{k}_B\right)$$

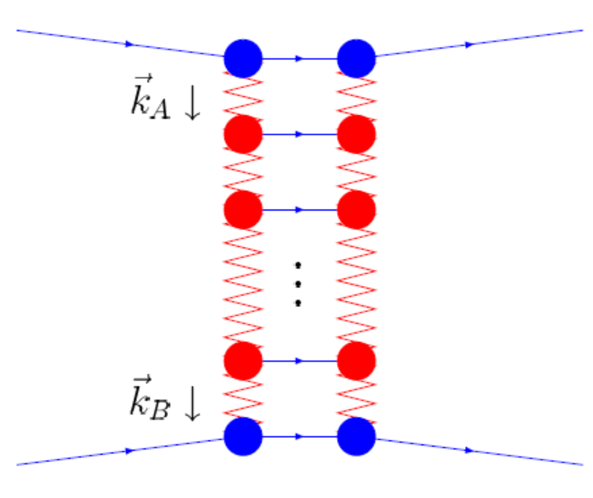

$$\varphi\left(\vec{k}_A, \vec{k}_B, \mathrm{Y}\right) = e^{2\,\omega_0\left(-\vec{k}_A^2\right)\mathrm{Y}}\Bigg[\delta^{(2)}\left(\vec{k}_A - \vec{k}_B\right)$$

$$+\sum_{n=1}^{\infty}\prod_{i=1}^{n}\bar{\alpha}_s\int\frac{d^2\vec{k}_i}{\pi\vec{k}_i^2}\theta\left(\vec{k}_i^2-\mu^2\right)\int_0^{y_{i-1}}dy_i\,e^{2\,\omega_0^{(i,i-1)}y_i}\delta^{(2)}\left(\vec{k}_A-\vec{k}_B+\sum_{l=1}^{n}\vec{k}_l\right)\Bigg]$$

$$\omega_0^{(i,i-1)} \equiv \omega_0\left(-\left(\vec{k}_A+\sum_{l=1}^{i}\vec{k}_l\right)^2\right)-\omega_0\left(-\left(\vec{k}_A+\sum_{l=1}^{i-1}\vec{k}_l\right)^2\right)$$

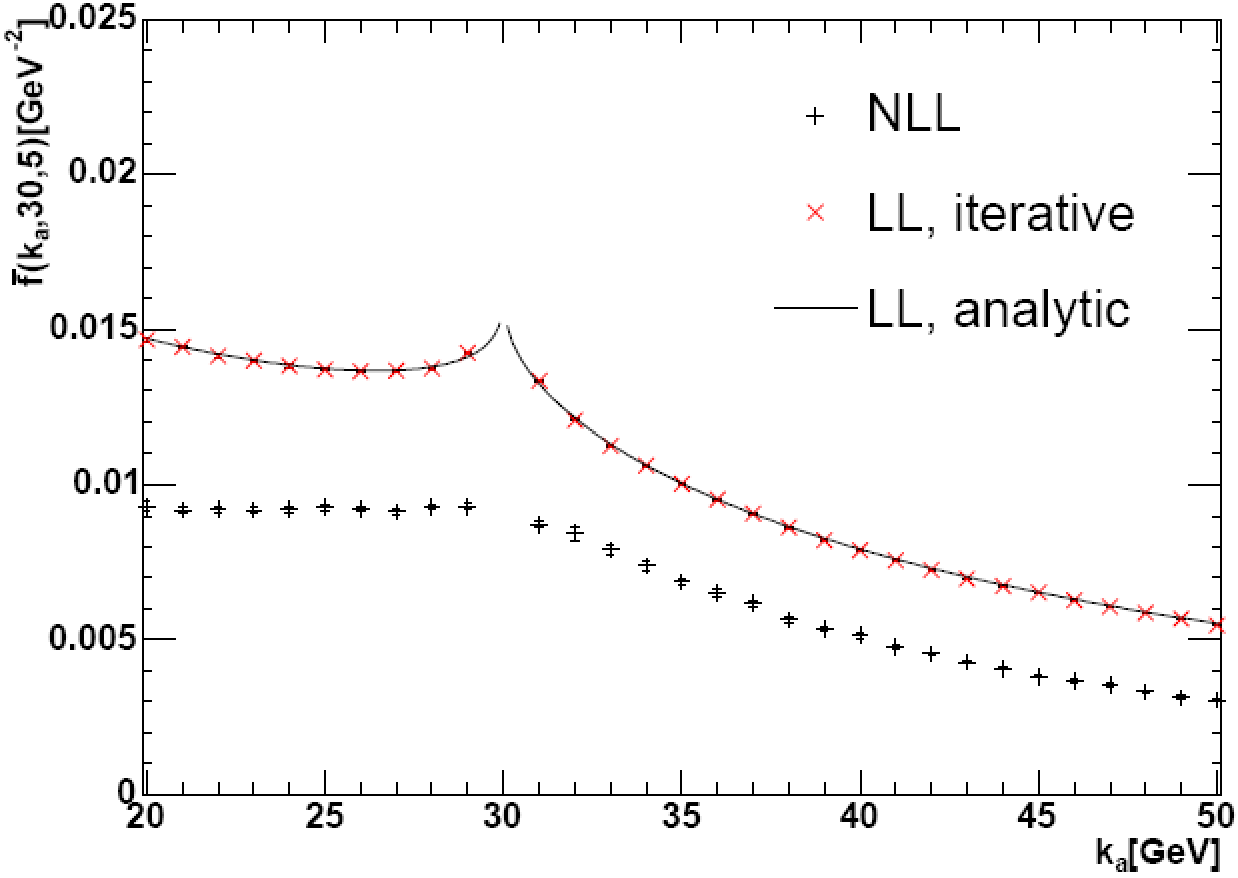

$\bar{f}(k_a,30,5)$[GeV^{-2}]
0.025
0.02
0.015
0.01
0.005
0
20
25
30
35
40
45
50
k_a[GeV]
NLL
LL, iterative
LL, analytic

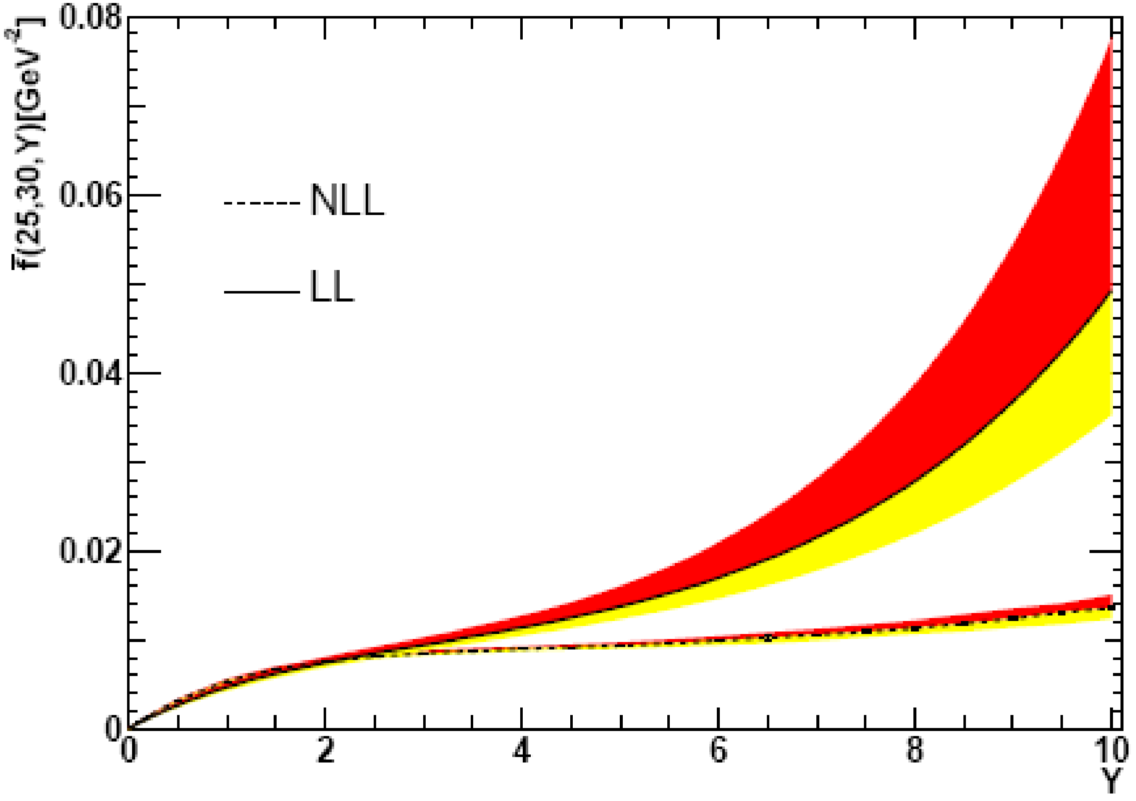

f̄(25,30,Y)[GeV^-2]
0.08
0.06
0.04
0.02
0
NLL
LL
0
2
4
6
8
10
Y

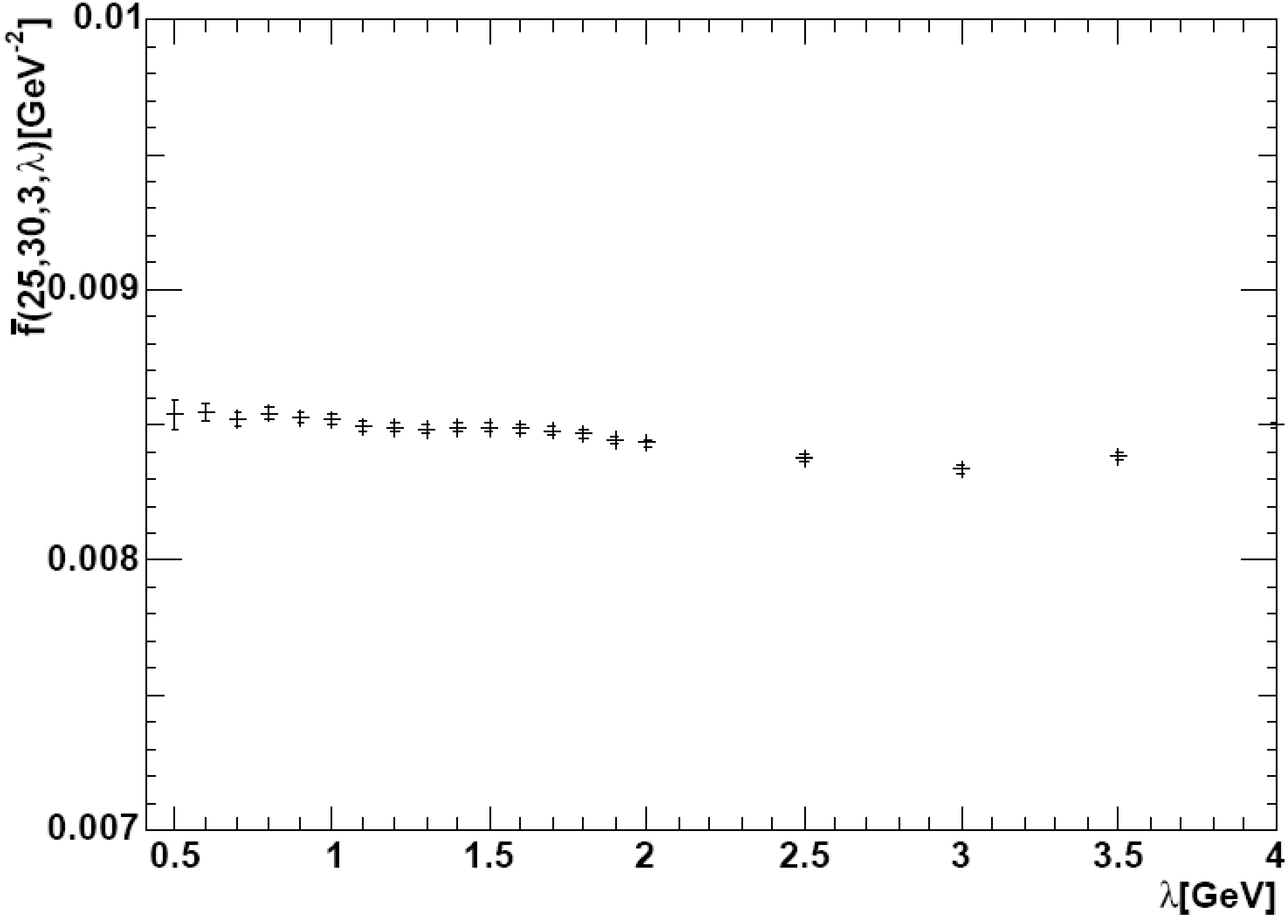

f̄(25,30,3,λ)[GeV^-2]
0.01
0.009
0.008
0.007
0.5
1
1.5
2
2.5
3
3.5
4
λ[GeV]

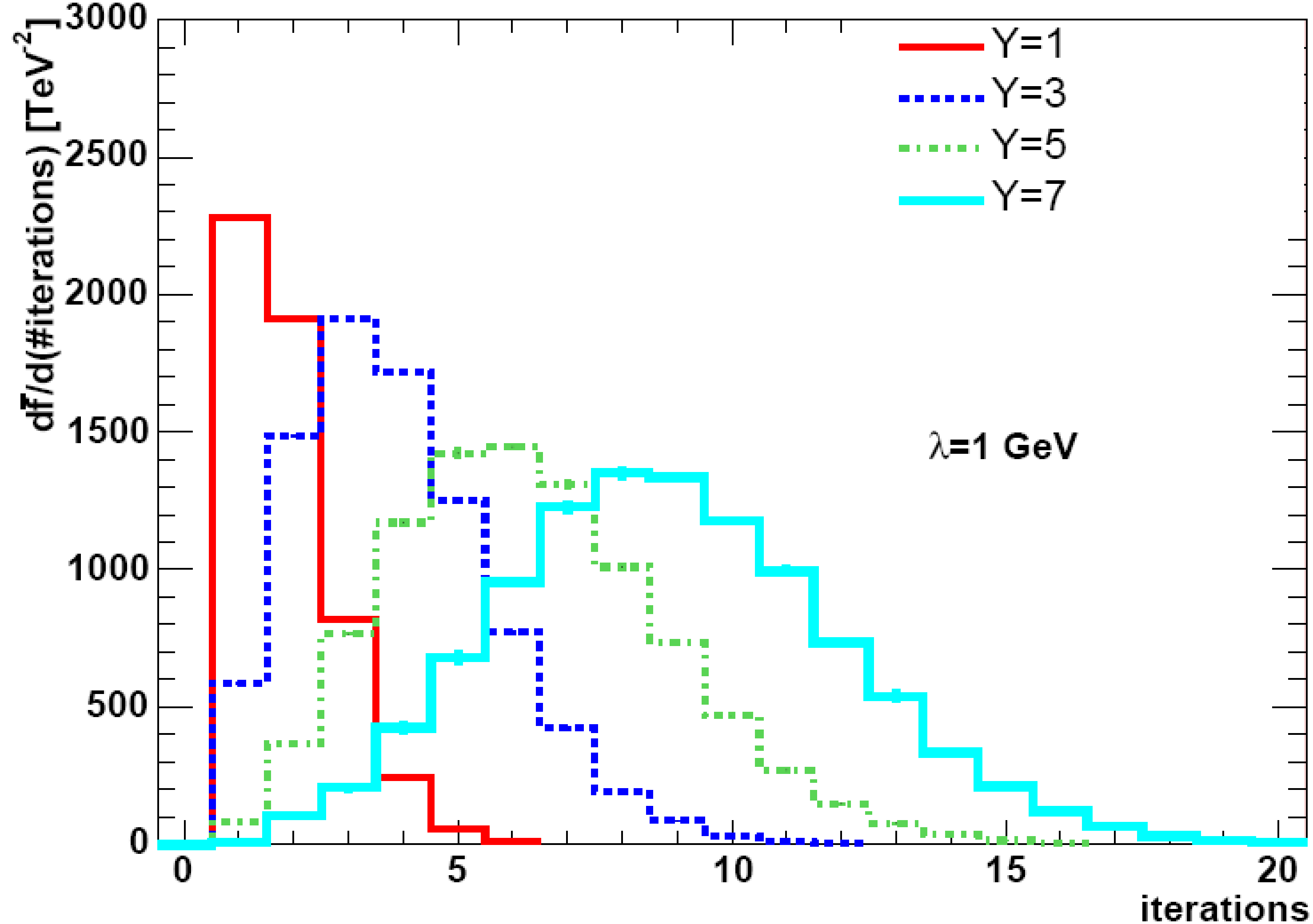

dσ̄/d(#iterations) [TeV^{-2}]
3000
2500
2000
1500
1000
500
0
0
5
10
15
20
iterations
Y=1
Y=3
Y=5
Y=7
λ=1 GeV

Diffusion into the infrared is cut–off by the momentum transfer, typical transverse momenta:

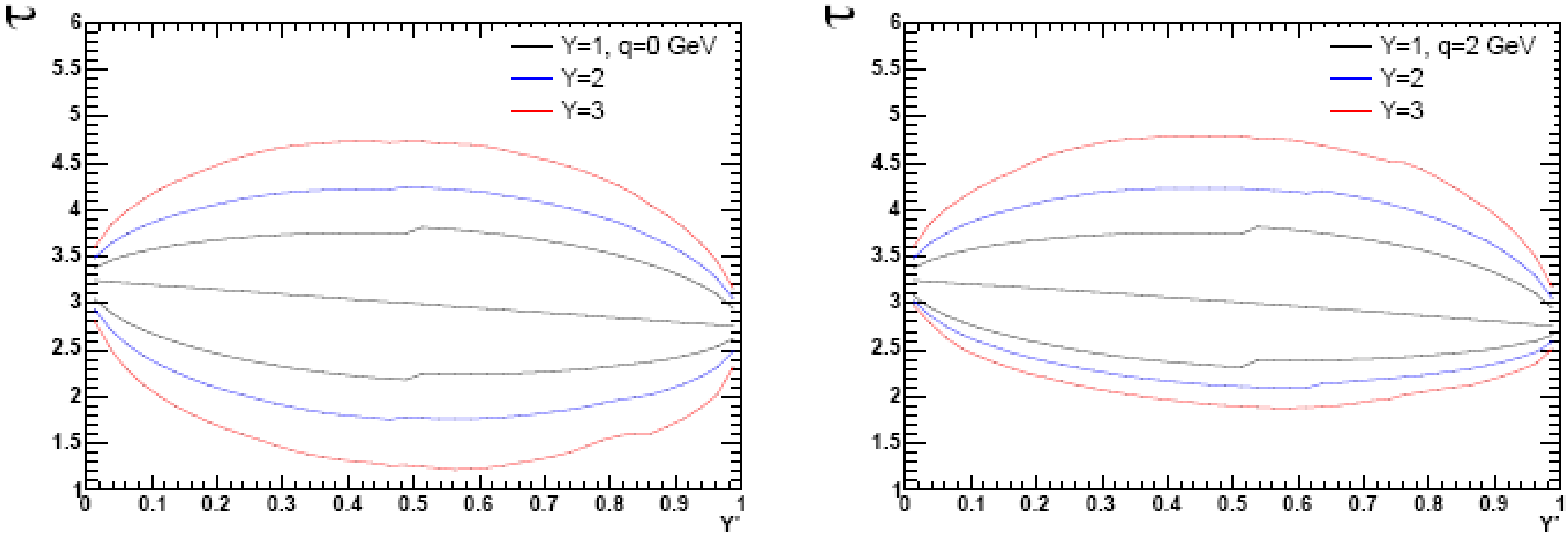

Forward case: Behaviour for small/large $\frac{k_a}{k_b}$ ratios:

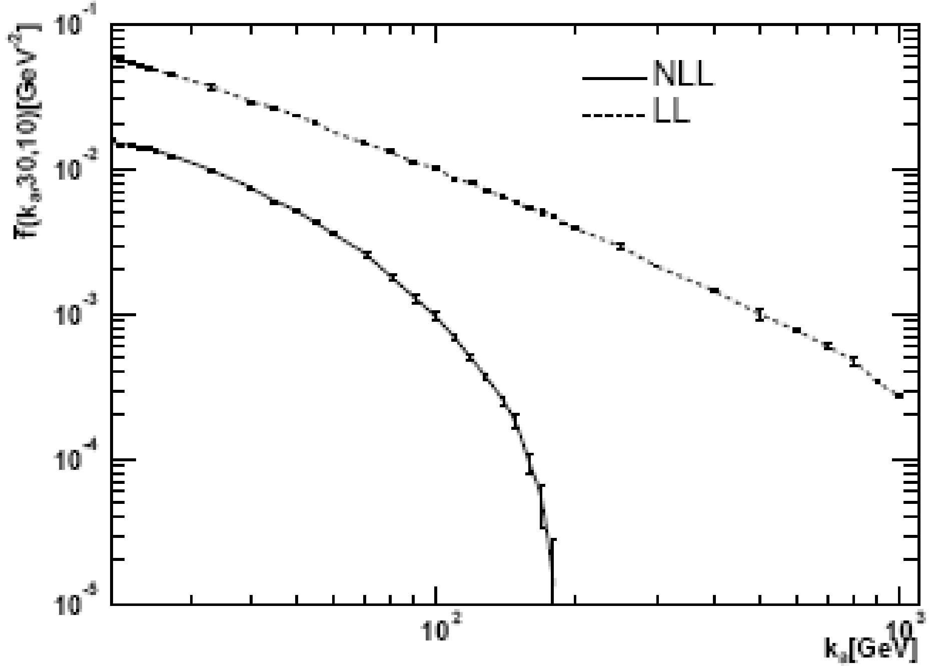

Collinear/Anticollinear limits: Oscillations

Origin of the oscillations: $\chi_0(\gamma) = \bar{\alpha}_s \left(2\Psi(1) - \Psi(\gamma) - \Psi(1-\gamma)\right)$

$$f \sim \int \left(\frac{s}{k_a k_b}\right)^{\omega} \left(\frac{\mathbf{k}_a^2}{\mathbf{k}_b^2}\right)^{\gamma - \frac{1}{2}} \frac{d\omega\, d\gamma}{\omega - \chi_0(\gamma)} = \int \left(\frac{s}{k_a^2}\right)^{\omega} \left(\frac{\mathbf{k}_a^2}{\mathbf{k}_b^2}\right)^{\gamma - \frac{1}{2}} \frac{d\omega\, d\gamma}{\omega - \chi_0(\gamma - \frac{\omega}{2})}$$

In collinear limit $\gamma \sim 0$: $\omega(\gamma) \sim \frac{\bar{\alpha}_s}{\gamma}$

$$\omega \sim \frac{\bar{\alpha}_s}{\gamma - \frac{\omega}{2}} \longrightarrow \omega \sim \frac{\bar{\alpha}_s}{\gamma} + \frac{\bar{\alpha}_s^2}{2\gamma^3} + \sum_{n=2}^{\infty} \frac{(2n)!}{2^n n!(n+1)!} \frac{\bar{\alpha}_s^{n+1}}{\gamma^{2n+1}}$$

Not allowed by DGLAP. Only the second one cancelled by NLL kernel.

The remaining terms are numerically large.

Proposal: $\chi_0^{\rm new}(\gamma) \equiv \chi_0\left(\gamma + \frac{\omega}{2}\right)$

$$f \sim \int \left(\frac{s}{k_a k_b}\right)^{\omega} \left(\frac{\mathbf{k}_a^2}{\mathbf{k}_b^2}\right)^{\gamma - \frac{1}{2}} \frac{d\omega\, d\gamma}{\omega - \chi_0(\gamma + \frac{\omega}{2})} = \int \left(\frac{s}{k_a^2}\right)^{\omega} \left(\frac{\mathbf{k}_a^2}{\mathbf{k}_b^2}\right)^{\gamma - \frac{1}{2}} \frac{d\omega\, d\gamma}{\omega - \chi_0(\gamma)}$$

Collinear limit free from unphysical double logs.

Main idea: the solution to

$$\omega = \bar{\alpha}_s \left(2\psi(1) - \psi\left(\gamma + \frac{\omega}{2}\right) - \psi\left(1 - \gamma + \frac{\omega}{2}\right)\right)$$

at small coupling can be approximated very well by

$$\omega = \int_0^1 \frac{dx}{1-x} \left\{ \left(x^{\gamma-1} + x^{-\gamma}\right) \sqrt{\frac{2\bar{\alpha}_s}{\ln^2 x}} J_1\left(\sqrt{2\bar{\alpha}_s \ln^2 x}\right) - 2\bar{\alpha}_s \right\}$$

Modification of original kernel is to remove the term $-\frac{\bar{\alpha}_s^2}{4}\frac{1}{(\mathbf{q}-\mathbf{k})^2}\ln^2\left(\frac{q^2}{k^2}\right)$ in the real emission kernel, $\mathcal{K}_r(\mathbf{q},\mathbf{k})$, and replace it with

$$\frac{1}{(\mathbf{q}-\mathbf{k})^2}\left(\frac{q^2}{k^2}\right)^{-\mathrm{b}\bar{\alpha}_s\frac{|k-q|}{k-q}}\sqrt{\frac{2\left(\bar{\alpha}_s+\mathrm{a}\,\bar{\alpha}_s^2\right)}{\ln^2\left(\frac{q^2}{k^2}\right)}}J_1\left(\sqrt{2\left(\bar{\alpha}_s+\mathrm{a}\,\bar{\alpha}_s^2\right)\ln^2\left(\frac{q^2}{k^2}\right)}\right)-\mathrm{M\ T}$$

$$J_1\left(\sqrt{2\bar{\alpha}_s\ln^2\left(\frac{q^2}{k^2}\right)}\right)\simeq\sqrt{\frac{\bar{\alpha}_s}{2}\ln^2\left(\frac{q^2}{k^2}\right)}$$

$$J_1\left(\sqrt{2\bar{\alpha}_s\ln^2\left(\frac{q^2}{k^2}\right)}\right)\simeq\left(\frac{2}{\pi^2\bar{\alpha}_s\ln^2\left(\frac{q^2}{k^2}\right)}\right)^{\frac{1}{4}}\cos\left(\sqrt{2\bar{\alpha}_s\ln^2\left(\frac{q^2}{k^2}\right)}-\frac{3\pi}{4}\right)$$

This generates a good collinear behaviour ...

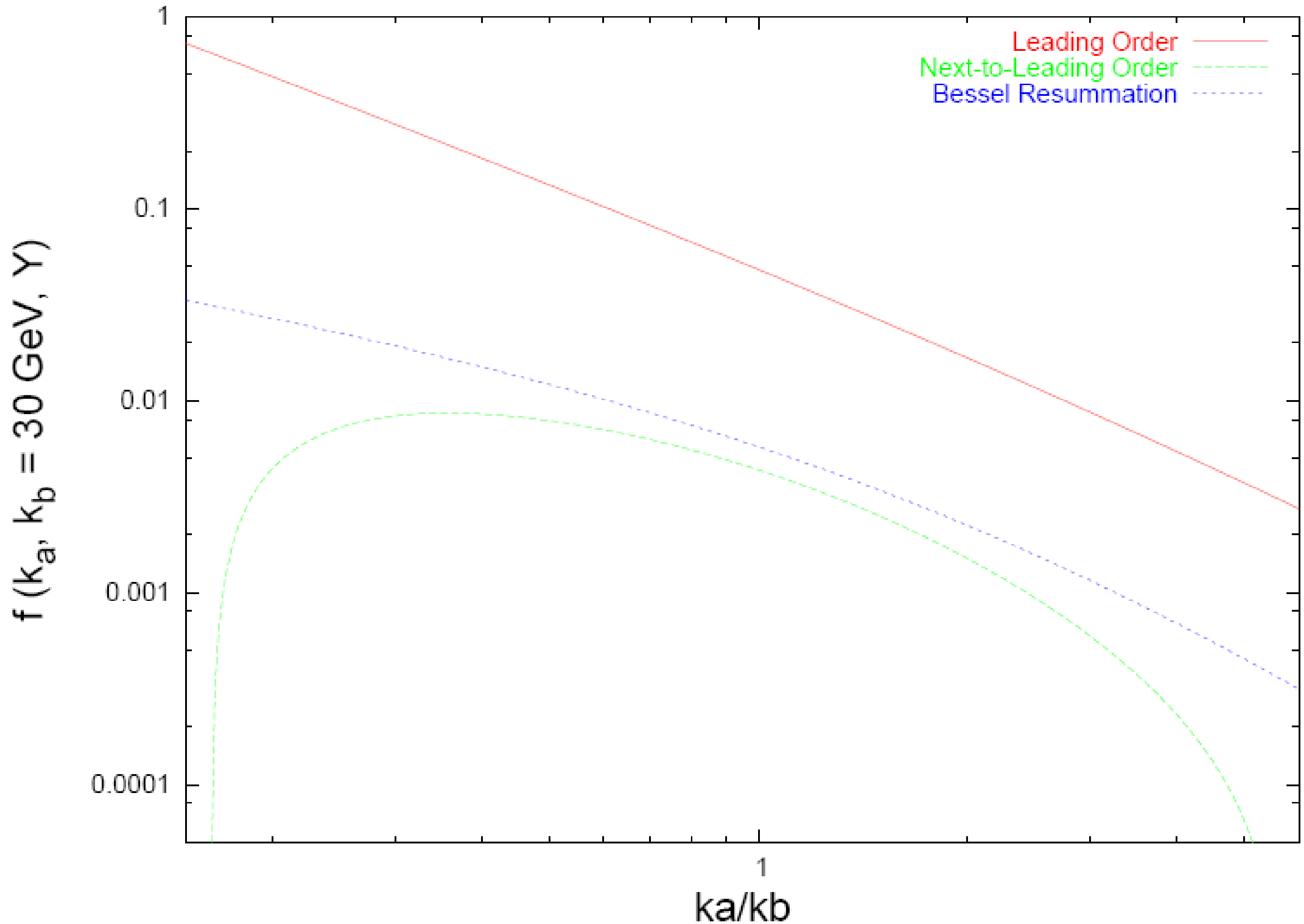

Leading Order
Next-to-Leading Order
Bessel Resummation
1
0.1
0.01
0.001
0.0001
1
f (k_a, k_b = 30 GeV, Y)
ka/kb

3. Vector meson production

Caporale, Papa, SV, Eur Phys J C(2008)

Collinear improvement of the BFKL kernel in the electroproduction of two light vector mesons

We consider the production of two light vector mesons ($V = \rho^0, \omega, \phi$) in the collision of two virtual photons,

$$\gamma^*(p)\,\gamma^*(p') \to V(p_1)\,V(p_2)\;.$$

$$p^2 = -Q_1^2 \text{ and } (p')^2 = -Q_2^2 \qquad s \gg Q_{1,2}^2 \gg \Lambda_{QCD}^2$$

The forward amplitude in the BFKL approach

$$\mathcal{I}m_s\left(\mathcal{A}\right) = \frac{s}{(2\pi)^2}\int\frac{d^2\vec{q}_1}{\vec{q}_1^{\,2}}\Phi_1(\vec{q}_1, s_0)\int\frac{d^2\vec{q}_2}{\vec{q}_2^{\,2}}\Phi_2(-\vec{q}_2, s_0)\int\limits_{\delta-i\infty}^{\delta+i\infty}\frac{d\omega}{2\pi i}\left(\frac{s}{s_0}\right)^{\omega}G_\omega(\vec{q}_1, \vec{q}_2)$$

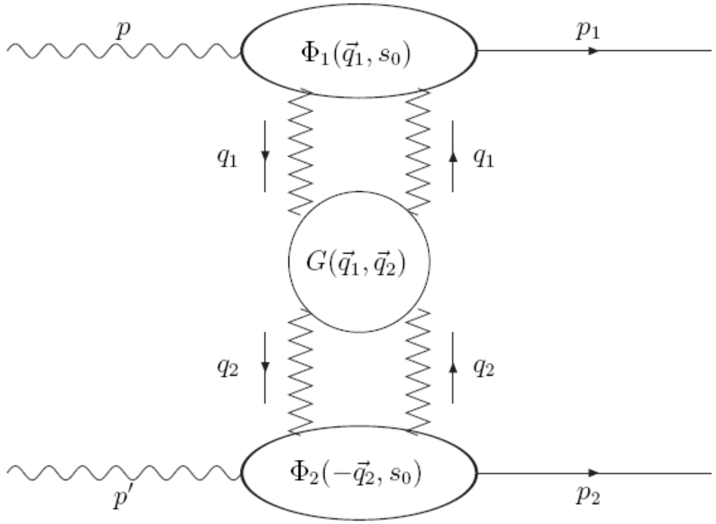

$$\hat{K}|\nu\rangle = \bar{\alpha}_s(\mu_R)\chi(\nu)|\nu\rangle + \bar{\alpha}_s^2(\mu_R)\left(\chi^{(1)}(\nu) + \frac{\beta_0}{4N_c}\chi(\nu)\ln(\mu_R^2)\right)|\nu\rangle$$
$$+ \bar{\alpha}_s^2(\mu_R)\frac{\beta_0}{4N_c}\chi(\nu)\left(i\frac{\partial}{\partial\nu}\right)|\nu\rangle + \chi_{RG}(\nu)|\nu\rangle$$

$$\chi_{RG}(\nu) = 2\Re e\left\{\sum_{m=0}^{\infty}\left[\left(\sum_{n=0}^{\infty}\frac{(-1)^n(2n)!}{2^n n!(n+1)!}\frac{(\bar{\alpha}_s + \mathrm{a}\,\bar{\alpha}_s^2)^{n+1}}{(1/2+i\nu+m-\mathrm{b}\,\bar{\alpha}_s)^{2n+1}}\right)\right.\right.$$
$$\left.\left. - \frac{\bar{\alpha}_s}{1/2+i\nu+m} - \bar{\alpha}_s^2\left(\frac{\mathrm{a}}{1/2+i\nu+m} + \frac{\mathrm{b}}{(1/2+i\nu+m)^2} - \frac{1}{2(1/2+i\nu+m)^3}\right)\right]\right\}$$

$$\mathrm{a} = \frac{5}{12}\frac{\beta_0}{N_c} - \frac{13}{36}\frac{n_f}{N_c^3} - \frac{55}{36}, \qquad \mathrm{b} = -\frac{1}{8}\frac{\beta_0}{N_c} - \frac{n_f}{6N_c^3} - \frac{11}{12}$$

$$\frac{\mathcal{I}m_s(\mathcal{A})}{D_1 D_2} = \frac{s}{(2\pi)^2}\int_{-\infty}^{+\infty} d\nu \left(\frac{s}{s_0}\right)^{\bar{\alpha}_s(\mu_R)\chi(\nu)+\bar{\alpha}_s^2(\mu_R)\left(\bar{\chi}(\nu)+\frac{\beta_0}{8N_c}\chi(\nu)\left[-\chi(\nu)+\frac{10}{3}\right]\right)+\chi_{RG}(\nu)} \alpha_s^2(\mu_R)c_1(\nu)c_2(\nu)$$
$$\times\left[1 + \bar{\alpha}_s(\mu_R)\left(\frac{c_1^{(1)}(\nu)}{c_1(\nu)} + \frac{c_2^{(1)}(\nu)}{c_2(\nu)}\right) + \bar{\alpha}_s^2(\mu_R)\ln\left(\frac{s}{s_0}\right)\frac{\beta_0}{8N_c}\chi(\nu)\left(i\frac{d\ln(\frac{c_1(\nu)}{c_2(\nu)})}{d\nu} + 2\ln(\mu_R^2)\right)\right]$$

$Q_1 = Q_2 \equiv Q$

optimal values $\mu_R \simeq 3Q$

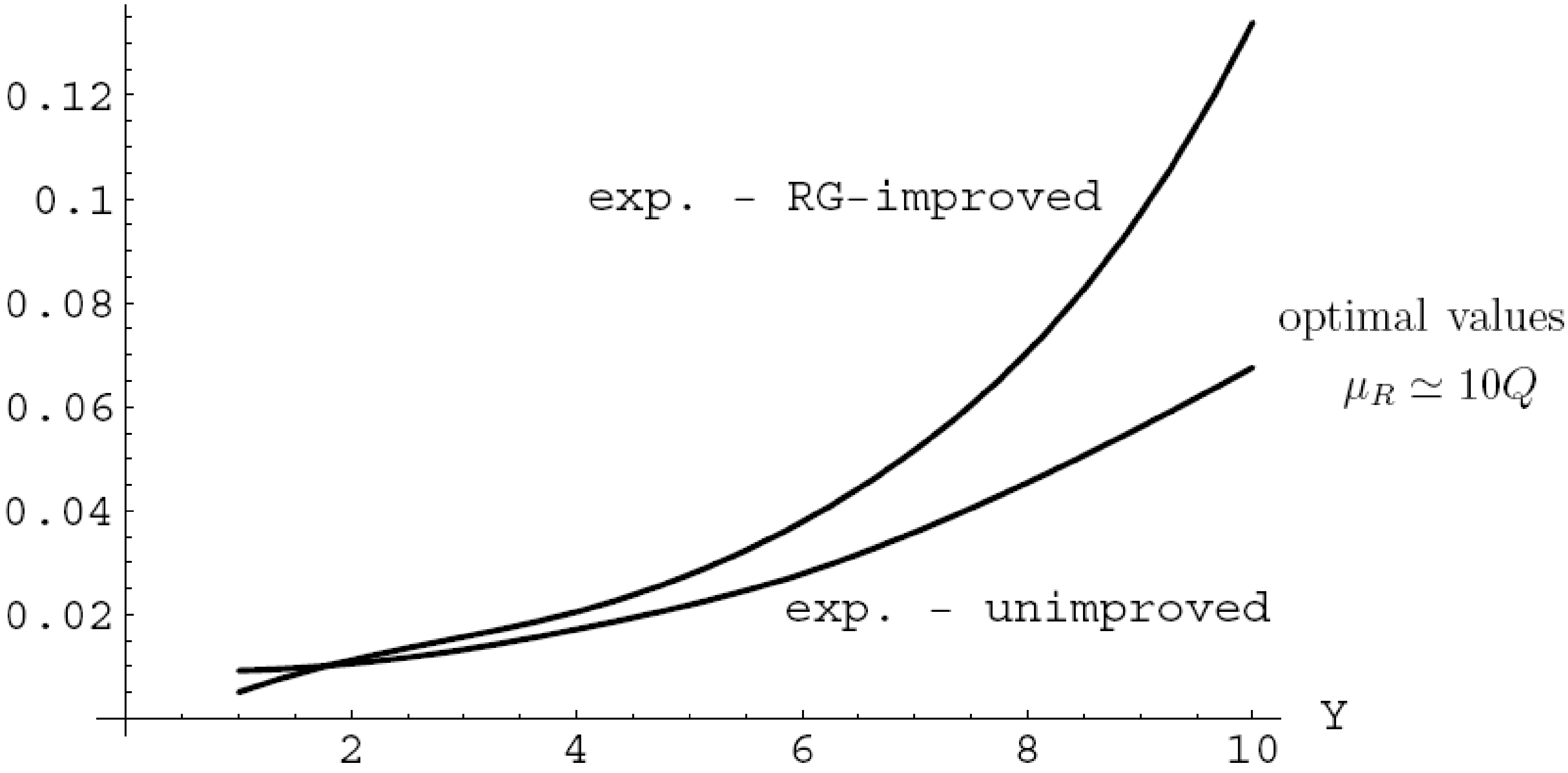

$\mathcal{I}m_s(\mathcal{A})Q^2/(s\,D_1 D_2)$ as a function of Y at Q^2=24 GeV^2

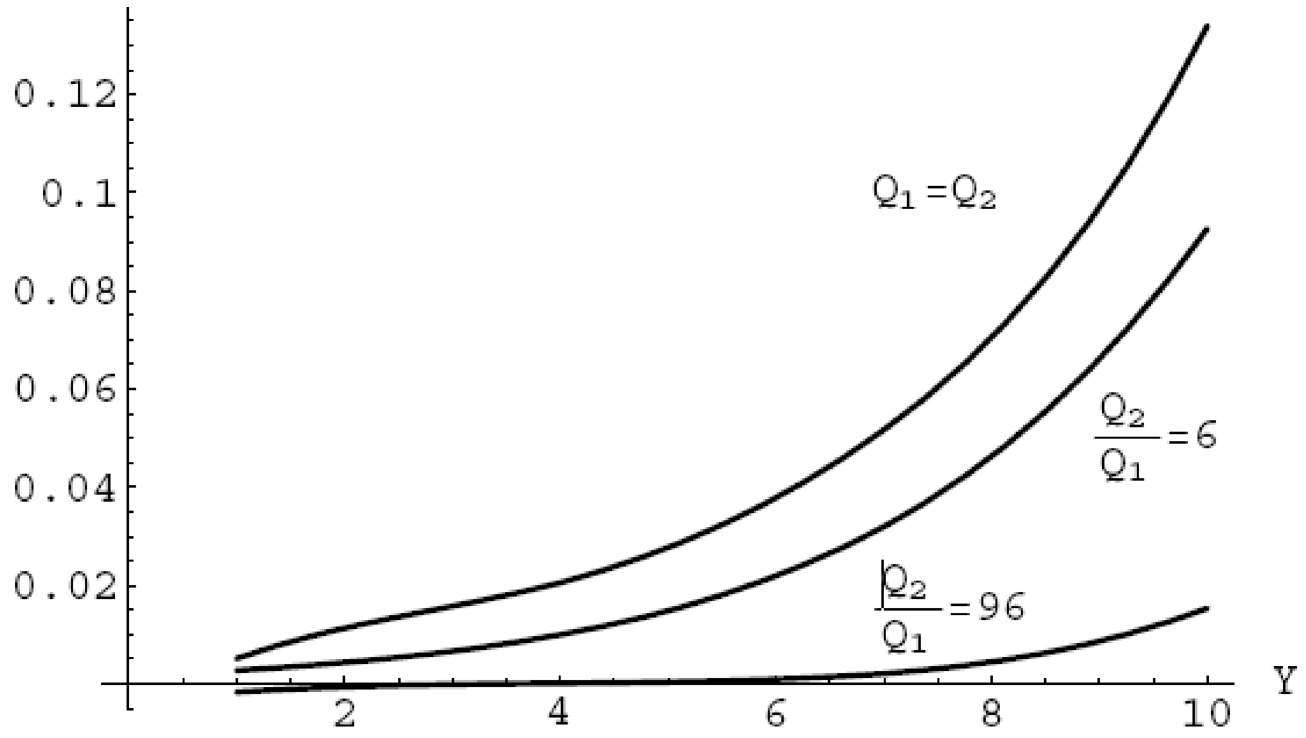

$\mathcal{I}m_s(\mathcal{A})Q_1Q_2/(s\,D_1D_2)$ as a function of Y for photons with strongly ordered virtualities ($Q_2/Q_1 = 6$ and $Q_2/Q_1 = 96$, with Q_1Q_2=24 GeV^2), in comparison with the case of photons with equal virtualities ($Q_1^2 = Q_2^2$=24 GeV^2).

4. Jet production: LHC & HERA

SV, NPB 722 (2005), NPB 746 (2006)

Bartels, SV, Schwennsen, JHEP 0611:051 (2006)

SV, Schwennsen, NPB 776 (2007)

SV, Schwennsen, PRD 77 (2008)

BFKL conformal structure can be identified in the azimuthal angle decorrelation of Mueller-Navelet jets

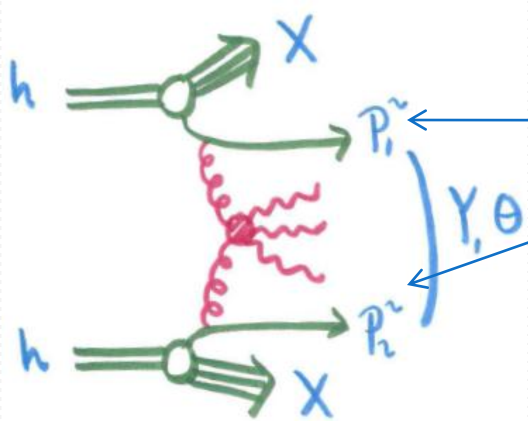

Tag most forward / backward jets with large and similar transverse momenta

Relative azimuthal angle / rapidity

Large center of mass energy

Project out the conformal components of the kernel with the observable:

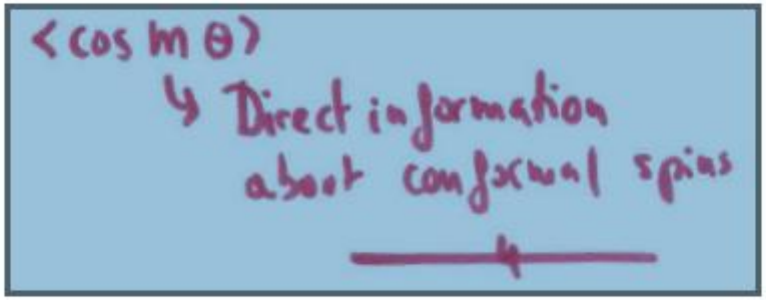

[Del Duca-Schmidt]

[Stirling]

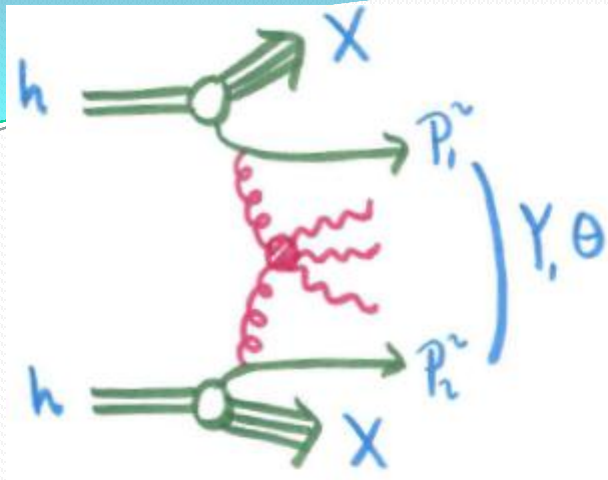

At small Y MN jets are back-to-back

At large Y more gluon emissions decorrelate the MN jets

Large difference between LO and higher order

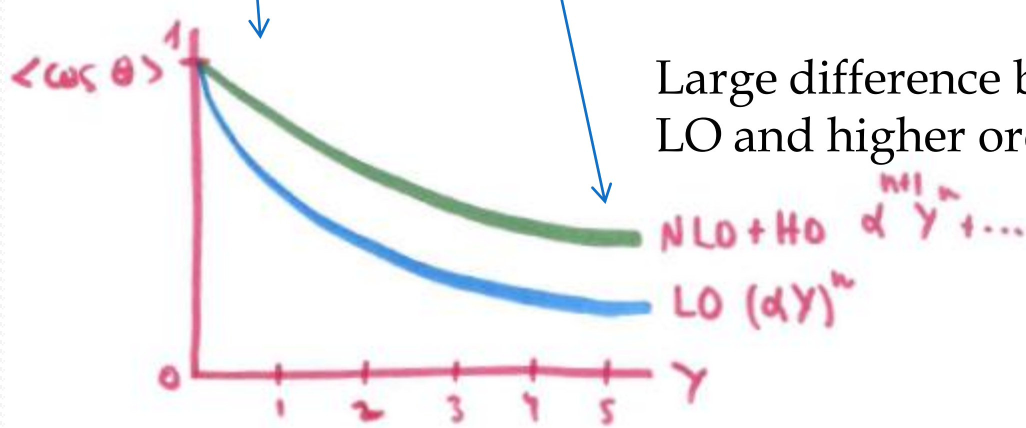

The ´perfect´ BFKL observable should remove the dependence on the zero conformal spin. This is the one most affected by collinear configurations not in original BFKL.

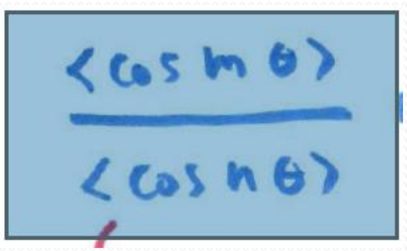

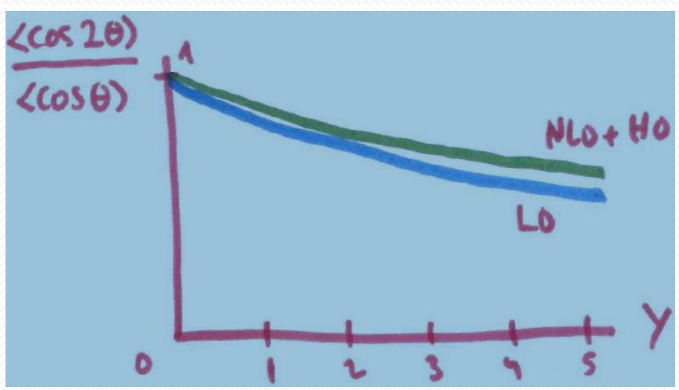

Small difference between LO and higher order calculations

Pythia and Herwig++ predict more correlation than BFKL

At the LHC we will go up to Y=12 and this observable will be measured

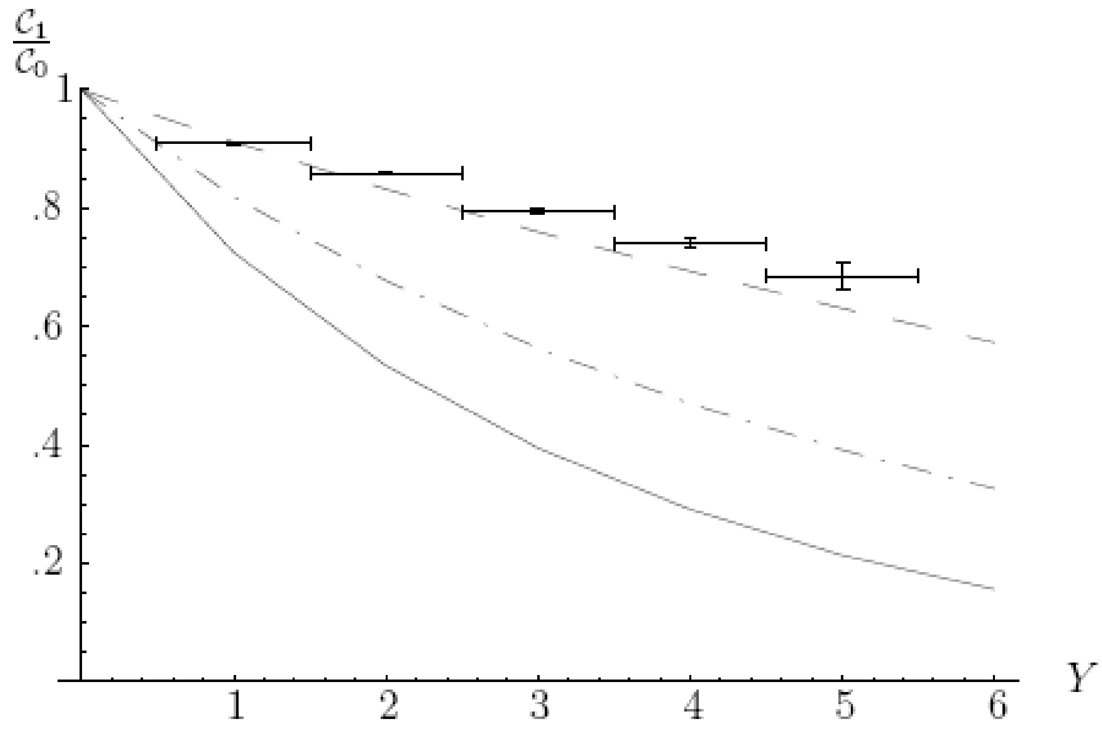

$\langle \cos\phi \rangle = \mathcal{C}_1/\mathcal{C}_0$ at a $p\bar{p}$ collider with $\sqrt{s} = 1.8$ TeV for BFKL at LO (solid) and NLO (dashed). The results from the resummation presented in the text are shown as well (dash–dotted).

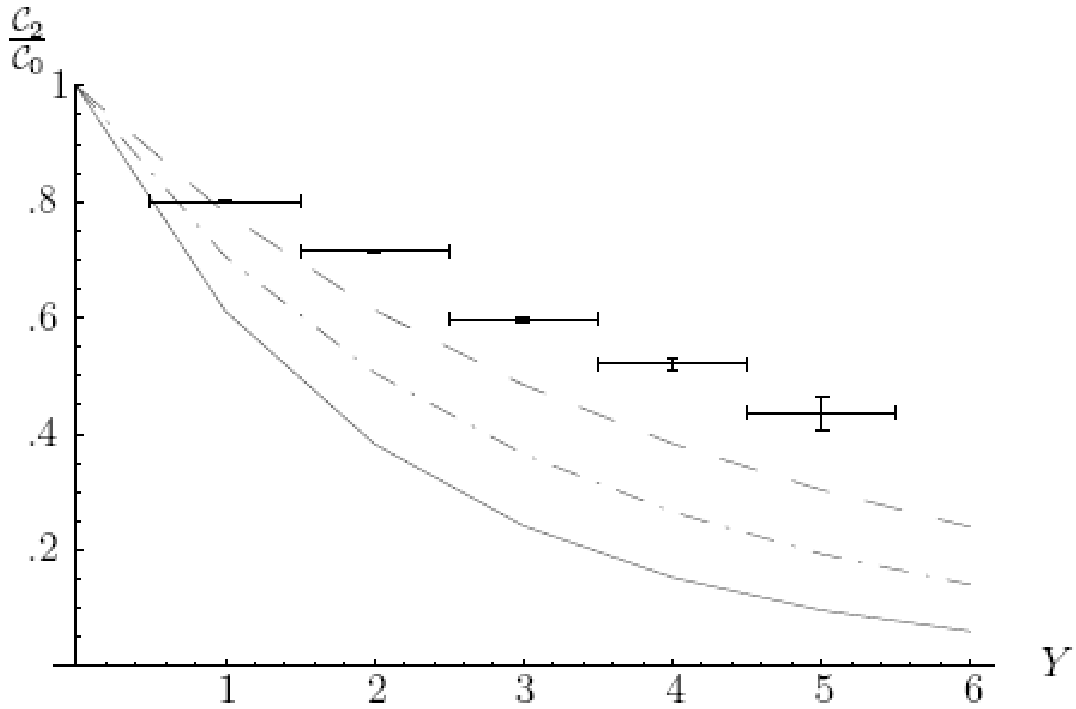

$\langle \cos 2\phi \rangle = \mathcal{C}_2/\mathcal{C}_0$ at a $p\bar{p}$ collider with $\sqrt{s} = 1.8$ TeV for BFKL at LO (solid) and NLO (dashed). The results from the resummation presented in the text are shown as well (dash–dotted).

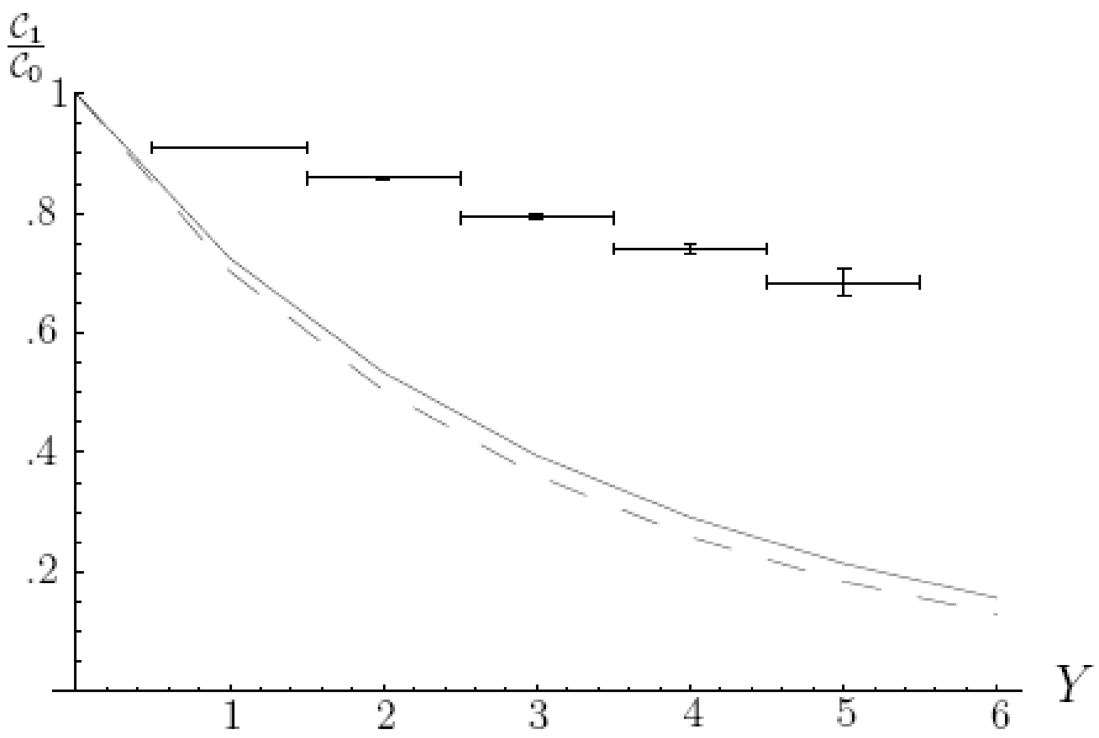

$\langle \cos\phi \rangle$ at LO comparing the $\overline{\text{MS}}$ renormalization scheme (solid) with the GB scheme (dashed).

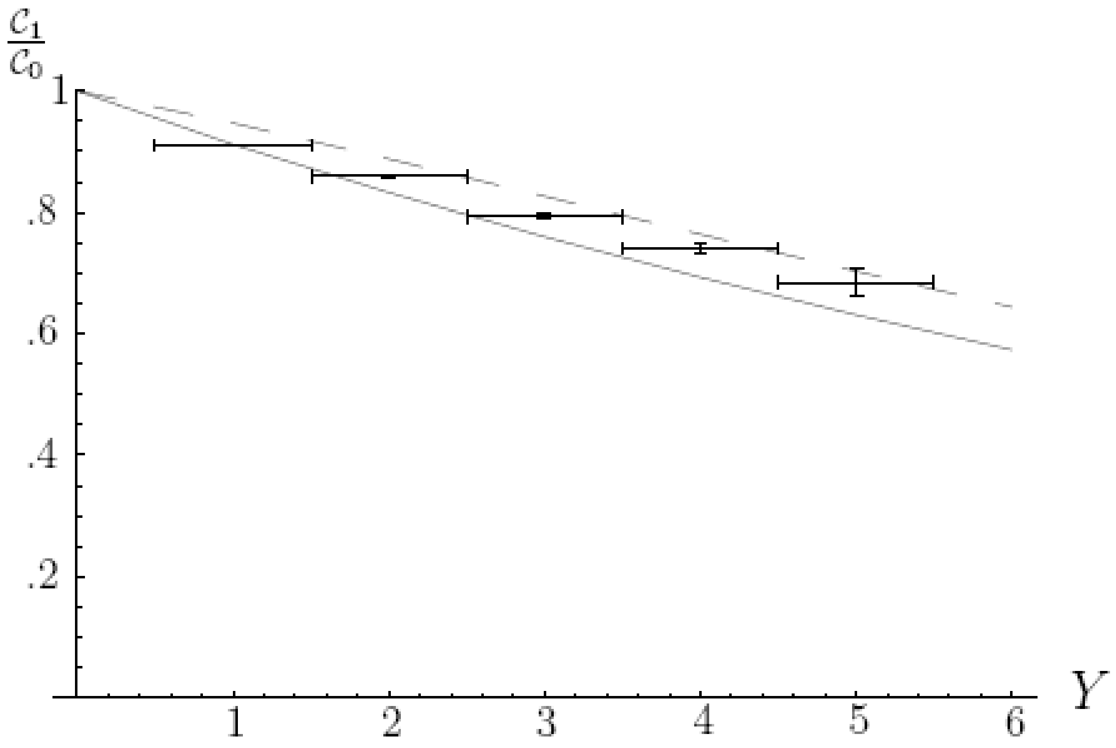

$\langle \cos\phi \rangle$ at NLO comparing the $\overline{\mathrm{MS}}$ renormalization scheme (solid) with the GB scheme (dashed).

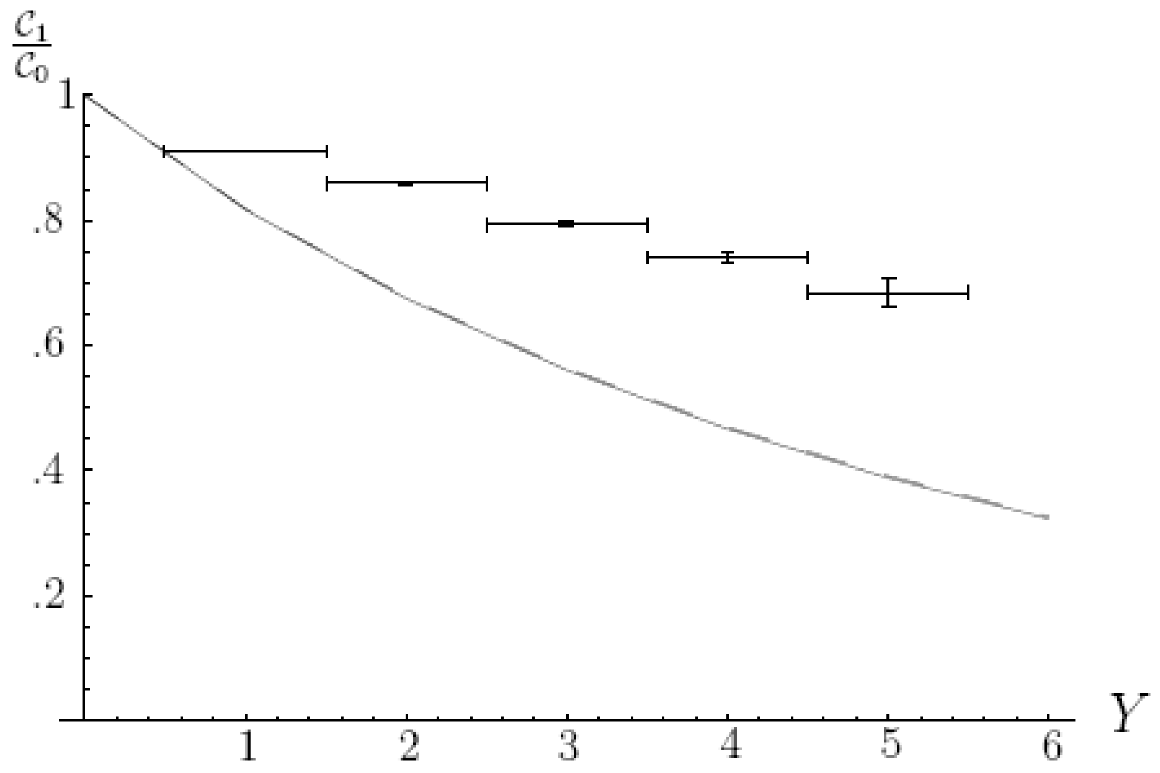

$\langle \cos\phi \rangle$ with a resummed kernel comparing the $\overline{\text{MS}}$ renormalization scheme (solid) with the GB scheme (dashed).

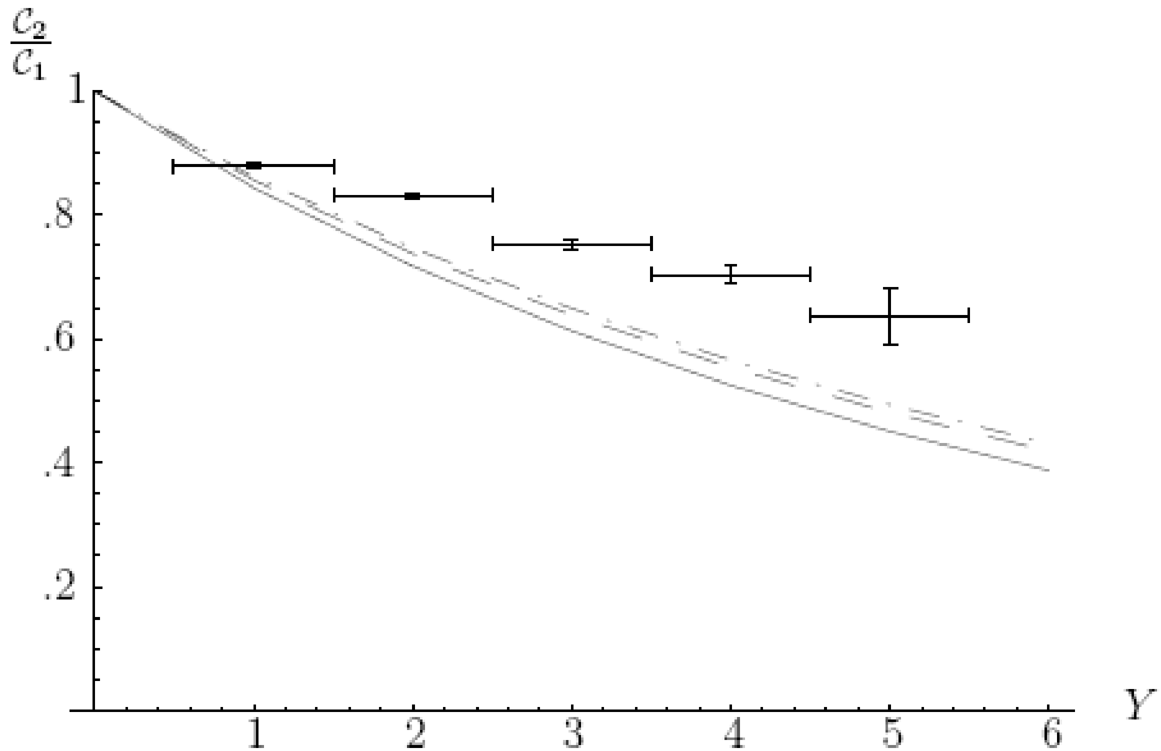

$\frac{<\cos 2\phi>}{<\cos \phi>} = \frac{\mathcal{C}_2}{\mathcal{C}_1}$ with LO (solid), NLO (dashed) and collinearly resummed (dash-dotted) BFKL kernels.

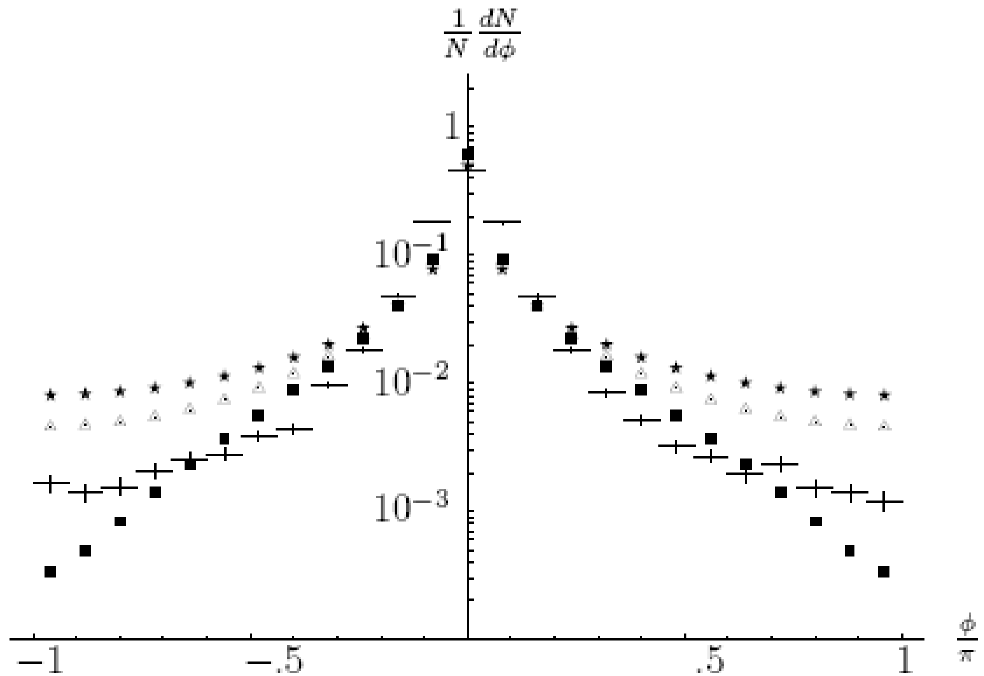

$\frac{1}{N}\frac{dN}{d\phi}$ in a $p\bar{p}$ collider at $\sqrt{s}$=1.8 TeV using a LO (stars), NLO (squares) and resummed (triangles) BFKL kernel. This plot is for Y = 1.

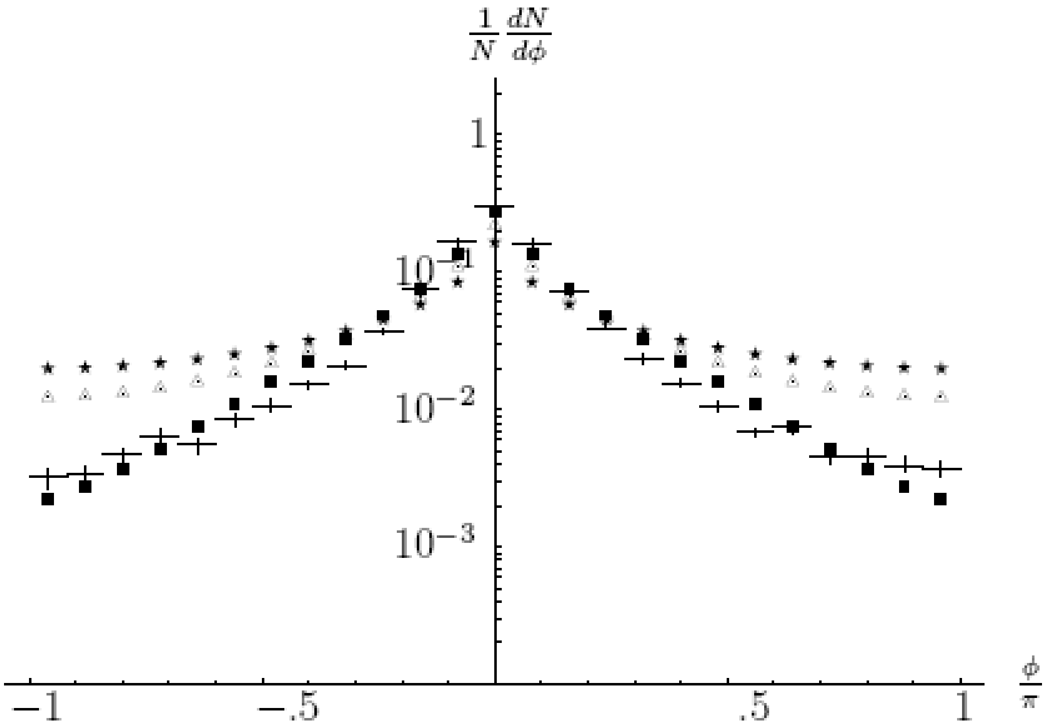

$\frac{1}{N}\frac{dN}{d\phi}$ in a $p\bar{p}$ collider at $\sqrt{s}$=1.8 TeV using a LO (stars), NLO (squares) and resummed (triangles) BFKL kernel. This plot is for Y = 3.

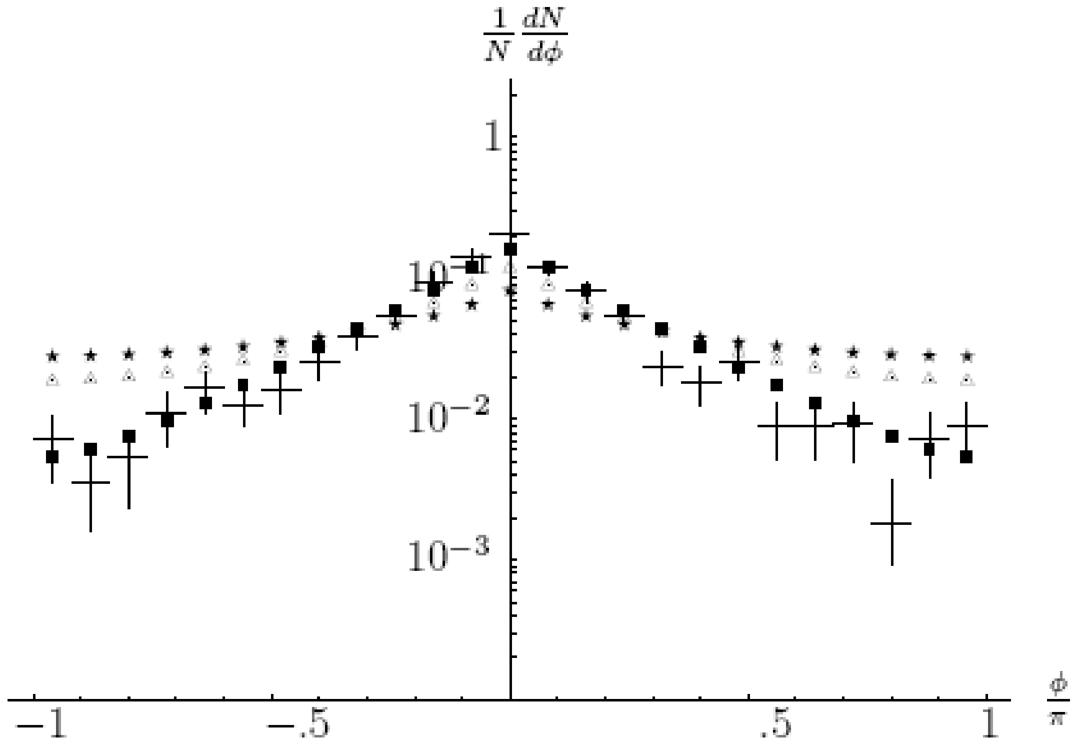

$\frac{1}{N}\frac{dN}{d\phi}$ in a $p\bar{p}$ collider at $\sqrt{s}$=1.8 TeV using a LO (stars), NLO (squares) and resummed (triangles) BFKL kernel. This plot is for Y = 5.

$$\sigma(s) = \int dx_{\rm FJ}\; f_{\rm eff}(x_{\rm FJ}, \mu_F^2)\hat{\sigma}(\hat{s})$$

$$f_{\rm eff}(x, \mu_F^2) = G(x, \mu_F^2) + \frac{4}{9}\sum_f \left[Q_f(x, \mu_F^2) + \bar{Q}_f(x, \mu_F^2)\right]$$

$$Q^2 = -q_\gamma^2$$

$$x_{\rm Bj} = \frac{Q^2}{2Pq_\gamma}$$

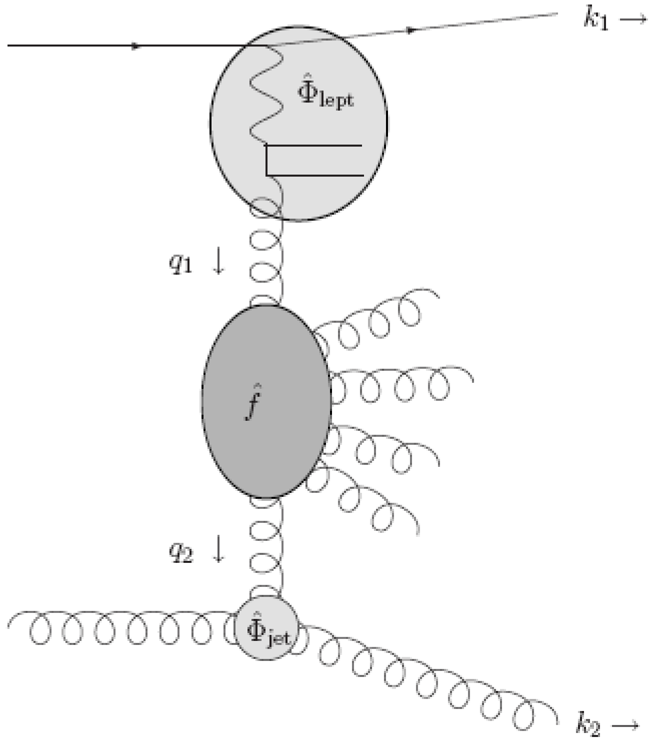

$$\mathbf{k}_1^2 = (1-y)Q^2$$

$$y = \frac{Pq_\gamma}{P(q_\gamma + k_1)}$$

$$Y = \ln x_{\rm FJ}/x_{\rm Bj}$$

$$\hat{\sigma}(\hat{s}) = \frac{\pi^2\bar{\alpha}_s^2}{2}\int d^2\mathbf{k}_1 \int d^2\mathbf{k}_2 \int \frac{d\omega}{2\pi i} e^{\omega Y} \langle \mathbf{k}_1 | \hat{\Phi}_{\rm leptonic} \hat{f}_\omega \hat{\Phi}_{\rm jet} | \mathbf{k}_2 \rangle$$

$$\langle \mathbf{q}_1|\nu,n\rangle = \frac{1}{\pi\sqrt{2}}\left(\mathbf{q}_1^2\right)^{i\nu-\frac{1}{2}} e^{in\theta_1} \qquad \hat{\mathcal{K}}_0|\nu,n\rangle = \bar{\alpha}_s\chi_0\left(|n|,\frac{1}{2}+i\nu\right)|\nu,n\rangle$$

$$\chi_0(n,\gamma) = 2\psi(1) - \psi\left(\gamma+\frac{n}{2}\right) - \psi\left(1-\gamma+\frac{n}{2}\right)$$

$$\hat{\sigma}(\hat{s}) = \frac{\pi^2\bar{\alpha}_s^2}{2}\sum_{n,n'=-\infty}^{\infty}\int d\alpha_1\int dy\int d^2\mathbf{k}_2\int\frac{d\omega}{2\pi i}\int d^2\mathbf{q}_1\int d^2\mathbf{q}_2\int d\nu\int d\nu'$$
$$\times\langle y,\alpha_1|\hat{\Phi}_{\rm leptonic}|\mathbf{q}_1\rangle\langle\mathbf{q}_1|\nu,n\rangle\langle n,\nu|\hat{f}_\omega|\nu',n'\rangle\langle n',\nu'|\mathbf{q}_2\rangle\langle\mathbf{q}_2|\hat{\Phi}_{\rm jet}|\mathbf{k}_2\rangle e^{\omega Y}$$

$$\text{ZEUS}: \qquad \frac{1}{2} < \frac{\mathbf{k}_2^2}{Q^2} < 2$$

$$\text{H1}: \qquad \frac{1}{2} < \frac{\mathbf{k}_2^2}{Q^2} < 5$$

$$\frac{1}{2}\int d\mathbf{k}_2^2\int d^2\mathbf{q}_2\,\langle n',\nu'|\mathbf{q}_2\rangle\langle\mathbf{q}_2|\hat{\Phi}_{\rm jet}|\mathbf{k}_2\rangle$$
$$=: c_2(\nu')\frac{e^{-in'\alpha_2}}{2\pi} = \frac{1}{\sqrt{2}}\frac{1}{\frac{1}{2}+i\nu'}\left(\frac{Q^2}{2}\right)^{-i\nu'-\frac{1}{2}}\left[1-\left(\frac{1}{4}\right)^{i\nu'-\frac{1}{2}}\right]\frac{e^{-in'\alpha_2}}{2\pi}$$

In the case of the H1 condition the 1/4 should be replaced for a 1/10

$$\int d^2\mathbf{q}_1 \langle y, \alpha_1 | \hat{\Phi}_{\text{leptonic}} | \mathbf{q}_1 \rangle \langle \mathbf{q}_1 | \nu, n \rangle$$

$$= \int dQ^2 \left[2A_1^{(0)}\left(\nu, y, Q^2\right) + A_1^{(2)}\left(\nu, y, Q^2\right) \left(\delta_{n,-2} e^{-2i\alpha_1} + \delta_{n,2} e^{2i\alpha_1}\right) \right]$$

$$\langle n, \nu | \hat{f} | \nu', n' \rangle = \int \frac{d\omega}{2\pi i} \langle n, \nu | \hat{f}_\omega | \nu', n' \rangle e^{\omega Y} = e^{\chi\left(|n|, \frac{1}{2} + i\nu, \bar{\alpha}_s\right) Y} \ \delta(\nu - \nu') \delta_{nn'}$$

$$\chi\left(n, \frac{1}{2} + i\nu, \bar{\alpha}_s\right) = \bar{\alpha}_s \chi_0\left(n, \frac{1}{2} + i\nu\right) + \bar{\alpha}_s^2 \left(\chi_1\left(n, \frac{1}{2} + i\nu\right) - \frac{\beta_0}{8N_c} \chi_0\left(n, \frac{1}{2} + i\nu\right) h_{\text{rc}}^{(n)}\left(\nu, y, Q^2\right)\right)$$

$$\frac{d\hat{\sigma}}{d\phi \ dy \ dQ^2} = \frac{\pi^2 \bar{\alpha}_s^2}{2} \left[B^{(0)}\left(y, Q^2, Y\right) + B^{(2)}\left(y, Q^2, Y\right) \cos 2\phi \right]$$

$$B_{\text{LO}}^{(n)}\left(y, Q^2, Y\right) = \int d\nu \ A^{(n)}\left(\nu, y, Q^2\right) \ c_2(\nu) e^{Y \bar{\alpha}_s \chi_0(|n|, \nu)}$$

$$B_{\text{NLO}}^{(n)}\left(y, Q^2, Y\right) = \int d\nu \ A^{(n)}\left(\nu, y, Q^2\right) \ c_2(\nu) \times e^{\bar{\alpha}_s(Q^2) \mathrm{Y}\left(\chi_0(|n|, \nu) + \bar{\alpha}_s(Q^2)\left(\chi_1(|n|, \nu) - \frac{\beta_0}{8N_c} \chi_0(n, \frac{1}{2} + i\nu) h_{\text{rc}}^{(n)}(\nu, y, Q^2)\right)\right)}$$

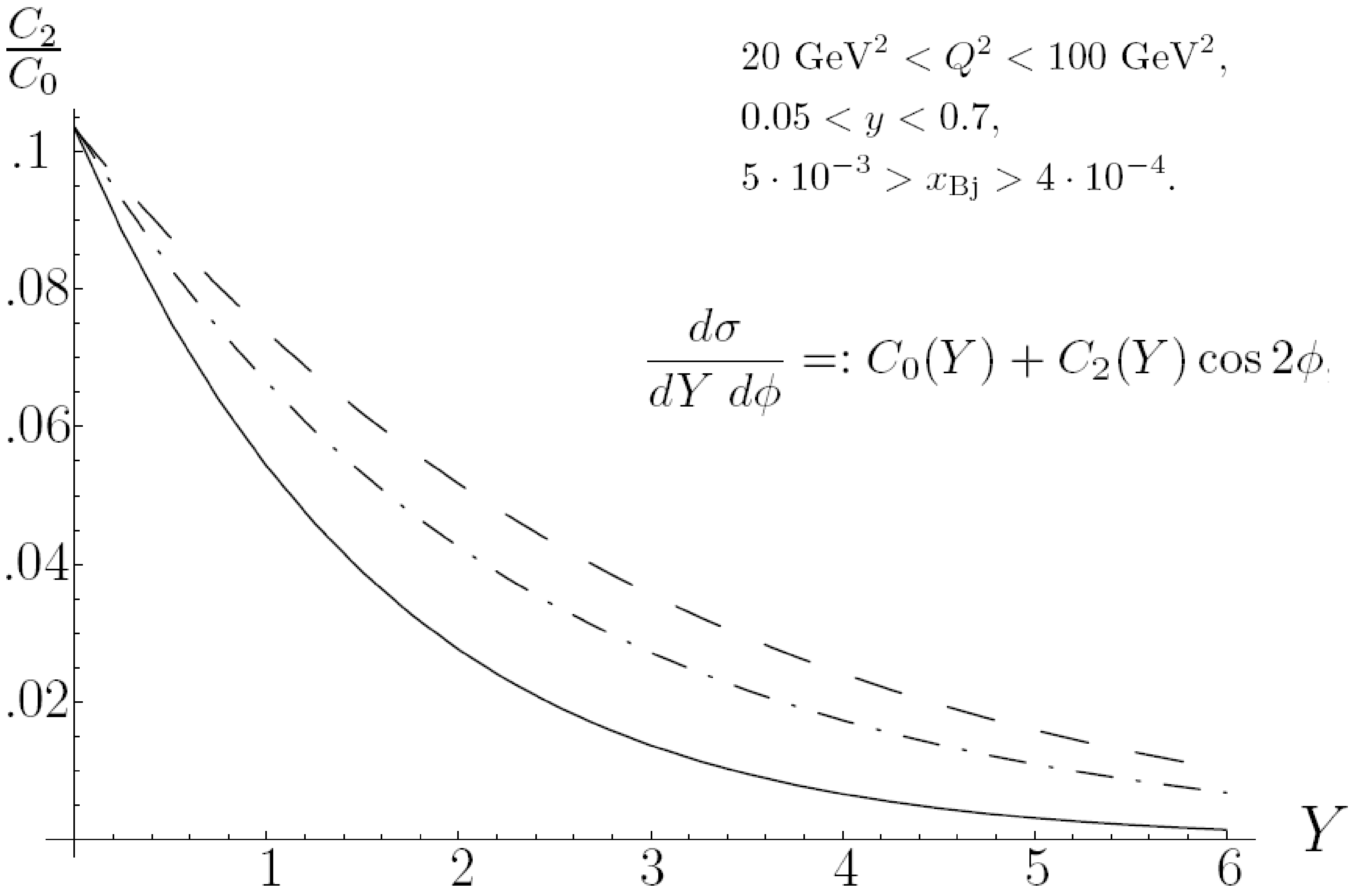
$\frac{C_2}{C_0}$
$20\ \mathrm{GeV}^2 < Q^2 < 100\ \mathrm{GeV}^2,$
$0.05 < y < 0.7,$
$5 \cdot 10^{-3} > x_{\mathrm{Bj}} > 4 \cdot 10^{-4}.$
$\frac{d\sigma}{dY\, d\phi} =: C_0(Y) + C_2(Y)\cos 2\phi$
.1
.08
.06
.04
.02
1
2
3
4
5
6
Y

5. Unitarity in DIS

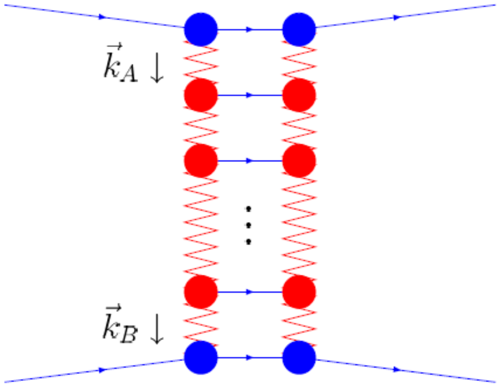

$$\bar{\varphi}(k_A, k_B, \mathrm{Y}) = \frac{1}{\pi k_A k_B} \int \frac{d\gamma}{2\pi i} \left(\frac{k_A^2}{k_B^2}\right)^{\gamma - \frac{1}{2}} e^{\chi(\gamma)\bar{\alpha}_s \mathrm{Y}}$$

At large energies the saddle point $\gamma = 1/2$ dominates

$$\chi(\gamma) \simeq 4 \log 2 + 14\, \zeta_3 \left(\gamma - \frac{1}{2}\right)^2 + \cdots$$

$$\bar{\varphi}(k_A, k_B, \mathrm{Y}) \simeq \frac{1}{2\pi k_A k_B} e^{\Delta \mathrm{Y}} \frac{1}{\sqrt{14\pi\zeta_3\bar{\alpha}_s \mathrm{Y}}} e^{\frac{-t^2}{56\zeta_3\bar{\alpha}_s \mathrm{Y}}}$$

with $t \equiv \log\left(k_A^2/k_B^2\right)$

IR/UV symmetric diffusion in transverse momenta for

$$\Phi(k_A, k_B, \mathrm{Y}) \equiv k_A\, k_B\, \bar{\varphi}(k_A, k_B, \mathrm{Y}) \qquad \frac{\partial \Phi}{\partial(\bar{\alpha}_s \mathrm{Y})} = 4\, \log 2\, \Phi + 14\, \zeta_3 \frac{\partial^2 \Phi}{\partial t^2}$$

$$\chi(\gamma) = 2\Psi(1) - \Psi(\gamma) - \Psi(1-\gamma)$$

$\gamma \to 1 - \gamma$ invariant

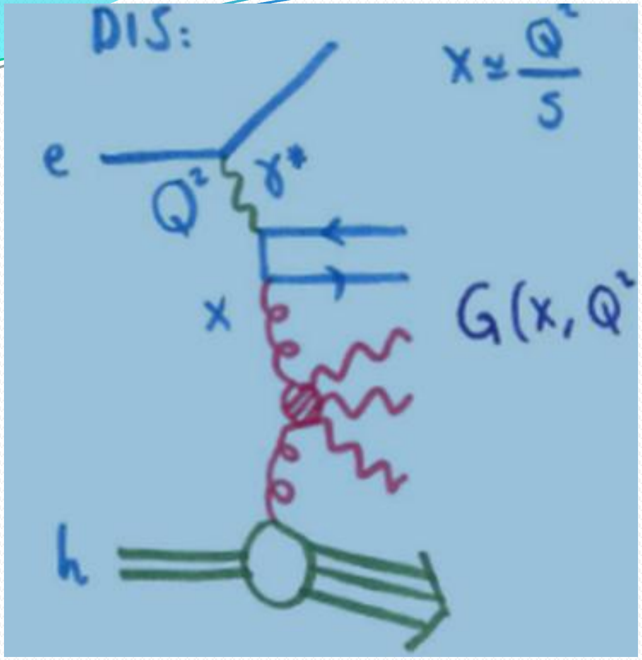

$$f(x, \mathbf{k}^2) \sim \left(\frac{x}{x_0}\right)^{-\lambda}$$ violates unitarity bounds

BFKL increases number of gluons of a fixed transverse size 1/Q

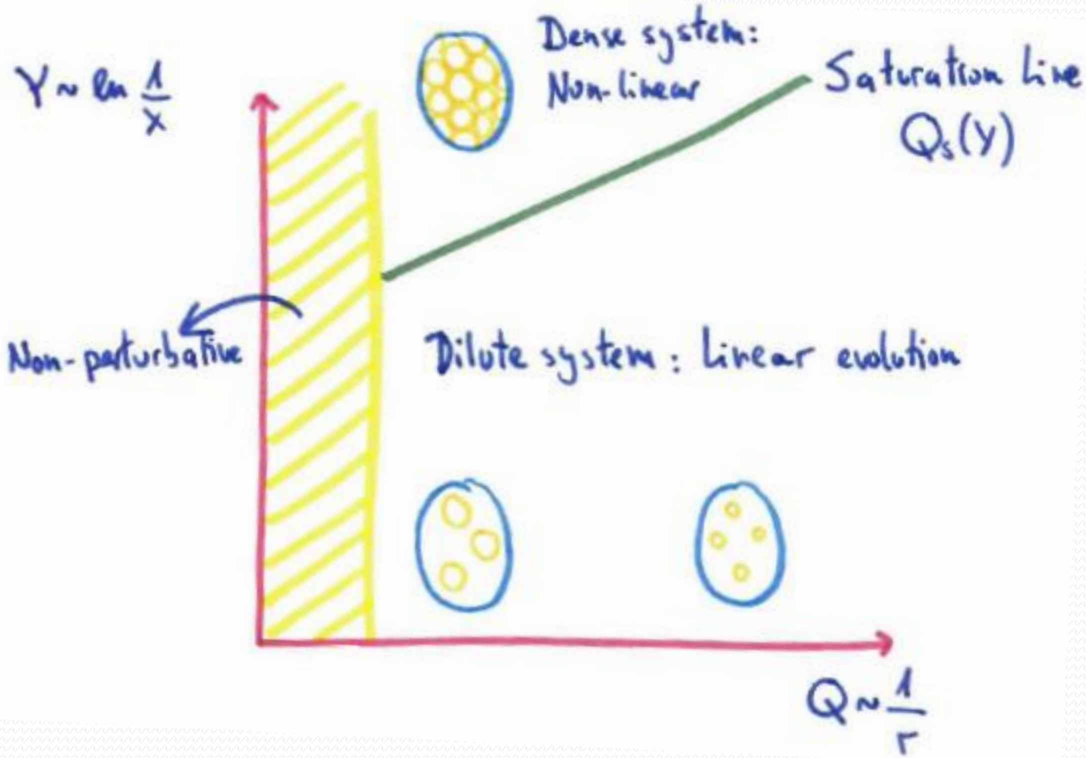

Perturbative degrees of freedom at high density dominated by nonlinearities

Non-linearities needed to damp this growth

For large targets BK equation is a good candidate:

$$\frac{\partial \Phi\left(k_A, k_B, \mathrm{Y}\right)}{\partial(\bar{\alpha}_s \mathrm{Y})} = -\Phi\left(k_A, k_B, \mathrm{Y}\right)^2 + \int_0^1 \frac{dx}{1-x}\left[\Phi\left(\sqrt{x} k_A, k_B, \mathrm{Y}\right) + \frac{1}{x}\Phi\left(\frac{k_A}{\sqrt{x}}, k_B, \mathrm{Y}\right) - 2\Phi\left(k_A, k_B, \mathrm{Y}\right)\right]$$

Non-linearities can be introduced with weighted diffusion in linear evolution:

$$\bar{\varphi}\left(Q_{\rm targ}, Q_{\rm proj}, \mathrm{Y}\right) = \frac{1}{\pi Q_{\rm targ}^2}\int \frac{d\gamma}{2\pi i}\left(\frac{Q_{\rm targ}^2}{Q_{\rm proj}^2}\right)^{\gamma} e^{\chi(\gamma)\bar{\alpha}_s \mathrm{Y}}$$

forced to have a different saddle point

$$\chi'(\gamma_0)\bar{\alpha}_s \mathrm{Y} + \log\left(\frac{Q_{\rm targ}^2}{Q_0^2}\right) = 0$$

$$\chi(\gamma) \simeq \chi(\gamma_0) + \chi'(\gamma_0)(\gamma - \gamma_0) + \frac{1}{2}\chi''(\gamma_0)(\gamma-\gamma_0)^2 + \cdots$$

$$\bar{\varphi}\left(Q_{\text{targ}}, Q_{\text{proj}}, \mathrm{Y}\right) \simeq e^{\gamma_0 t_0 + \bar{\alpha}_s \mathrm{Y}(\chi(\gamma_0) - \gamma_0 \chi'(\gamma_0))} \frac{e^{\frac{-t_0^2}{2\chi''(\gamma_0)\bar{\alpha}_s \mathrm{Y}}}}{\pi Q_{\text{targ}}^2 \sqrt{\chi''(\gamma_0) 2\pi \bar{\alpha}_s \mathrm{Y}}}$$

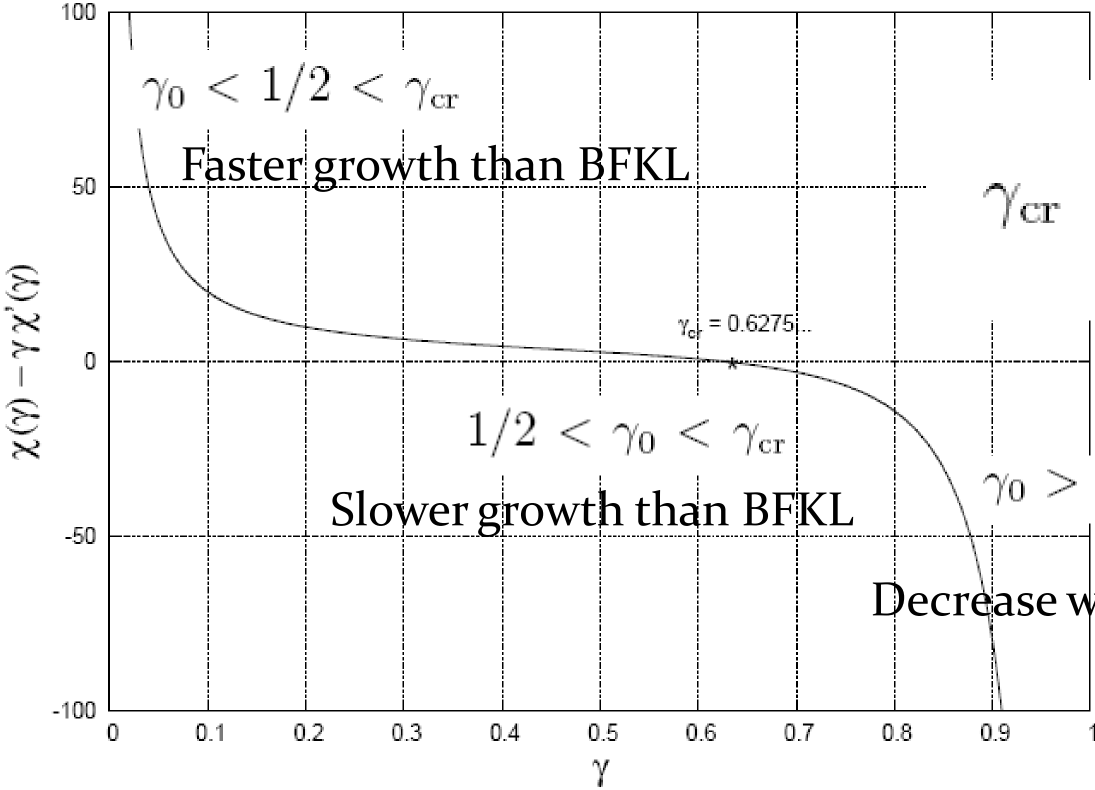

$\gamma_0 < 1/2 < \gamma_{cr}$

Faster growth than BFKL

$1/2 < \gamma_0 < \gamma_{cr}$

Slower growth than BFKL

$\gamma_0 > \gamma_{cr}$

Decrease with energy

$$\gamma_{cr} = \frac{\chi(\gamma_{cr})}{\chi'(\gamma_{cr})} \simeq 0.6275\ldots$$

For $\gamma_0 = \gamma_{cr}$ there is no growth with energy

$\gamma \to 1 - \gamma$

symmetry broken

$$\gamma_0 = \gamma_{cr}$$

IR suppression

$$\bar{\varphi}\left(Q_{targ}, Q_{proj}, Y\right) \simeq \left(\frac{Q_{cr}(Y)}{Q_{proj}}\right)^{2\gamma_{cr}} \frac{e^{\frac{-t_{cr}^2}{2\chi''(\gamma_{cr})\bar{\alpha}_s Y}}}{\pi Q_{targ}^2 \sqrt{\chi''(\gamma_{cr}) 2\pi\bar{\alpha}_s Y}}$$

Critical line: $$Q_{cr}(Y) = Q_{targ} \exp\left[\frac{\chi'(\gamma_{cr})}{2}\bar{\alpha}_s Y\right]$$

Solution invariant under geometrical scaling:

$$\bar{\alpha}_s Y \rightarrow \bar{\alpha}_s Y + \log\lambda,$$

$$\frac{Q_{proj}}{Q_{targ}} \rightarrow \frac{Q_{proj}}{Q_{targ}} \lambda^{\frac{\chi'(\gamma_{cr})}{2}}.$$

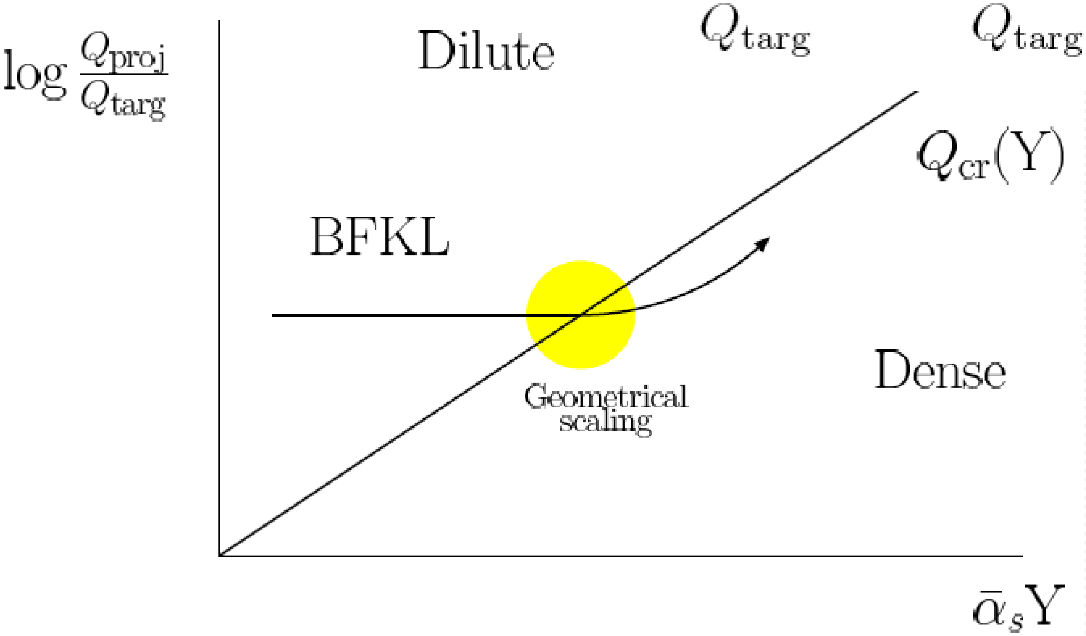

with critical exponent

$$\chi'(\gamma_{cr})/2 \simeq 2.4417...$$

for the crossover dilute-dense transition

Main features of saturation:

1. Dilute/dense transition
2. Scaling symmetry
3. Critical exponent 2.44
4. IR/UV competition

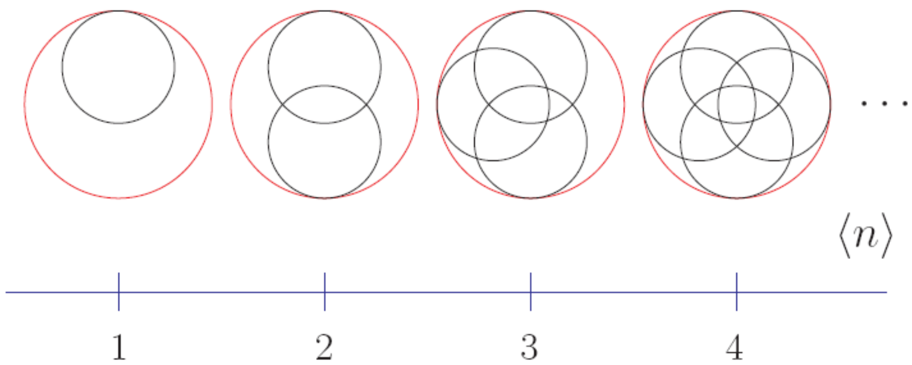

At asymptotic energies linear evolution has no memory on transverse sizes

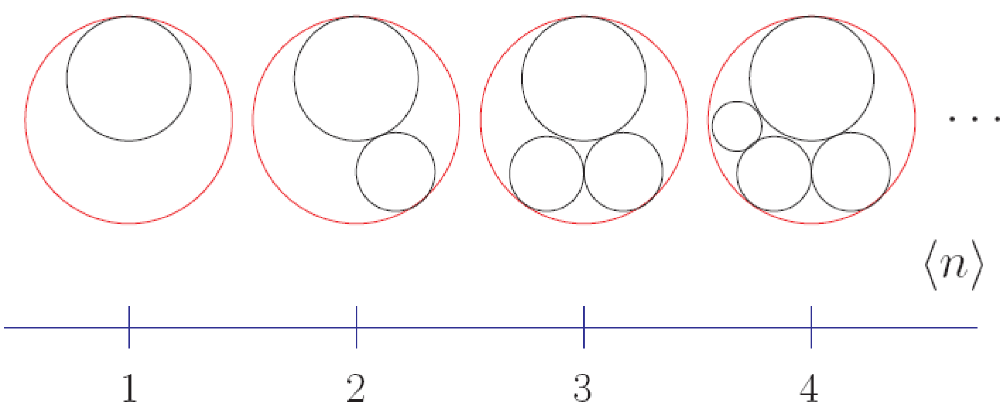

When memory is introduced infrared modes are suppressed

$$\mathcal{T}_{\rm cr} \;=\; \mathcal{T}_{\rm targ}\exp\left[-\frac{\chi'(\gamma_{\rm cr})}{2}\bar{\alpha}_s \mathrm{Y}\right]$$

LO BFKL:

- The coupling is fixed and carries colour factor

$$\bar{\alpha}_s \equiv \frac{\alpha_s(\mu) N_c}{\pi}, \ \mu \text{ is the } \overline{\text{MS}} \text{ scale.}$$

- No fermions
- The same kernel in all SUSY theories [Lipatov]
- Holomorphically separable and SL(2,C) invariant [Lipatov]
- Iterated in s-channel with periodic BC corresponds to an integrable Heisenberg ferromagnet. [Faddeev, Korchemsky]

Holographic interpretation at large coupling? [Brower-Polchinsky-Strassler-Tan] [Cornalba-Costa-Penedones]

Gravity dual of the saturation line? [Hatta-Iancu-Mueller]

$$Q_s(Y) = Q_0 \, e^{\bar{\alpha}_s Y \, 2.44}$$

Important: in the gauge theory side we are at small coupling

BFKL at NNLO:

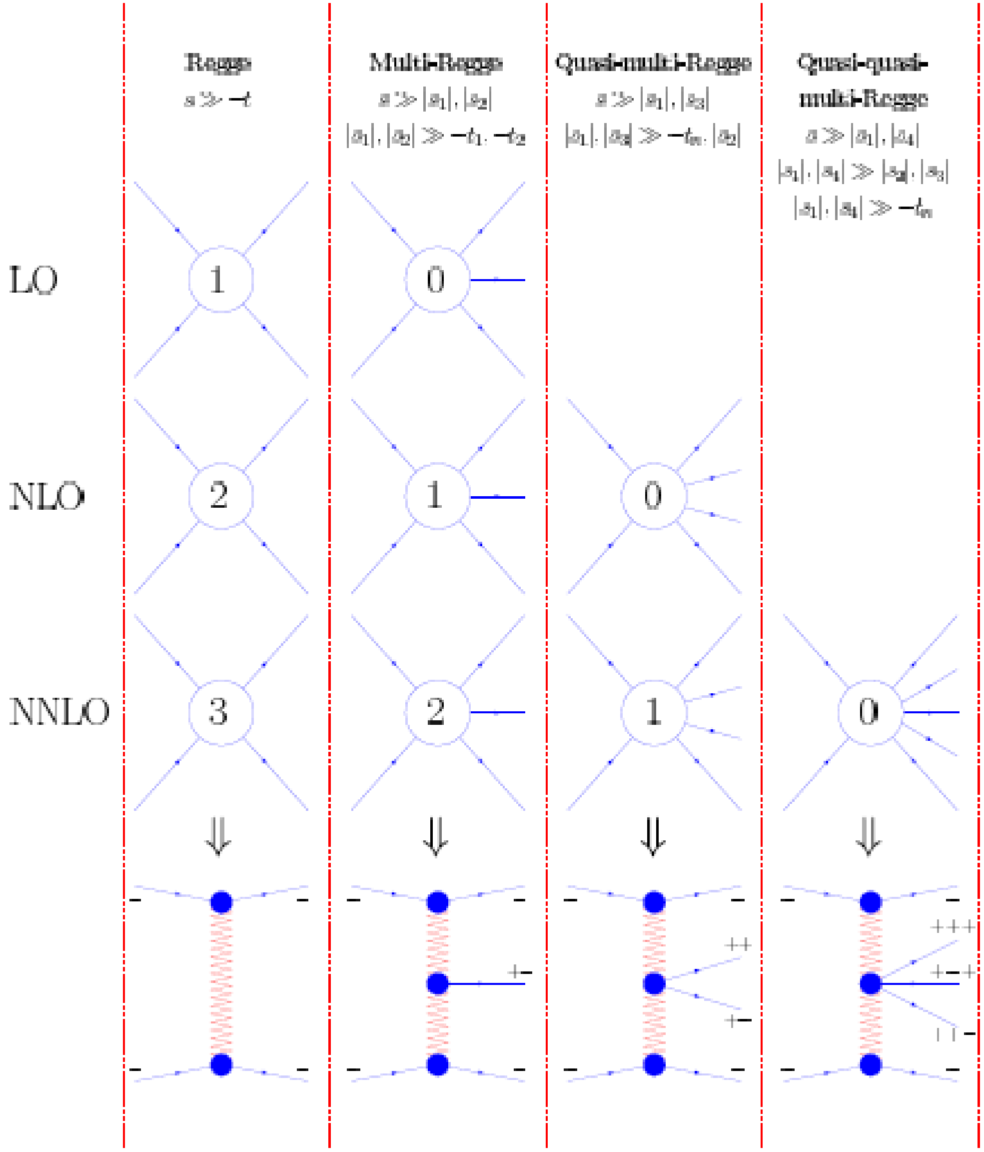

Diagrams contributing to the BFKL kernel in NNLLA

Use the ansatz by Bern, Dixon, Smirnov for N=4 SYM, MHV, planar amplitudes

[Bartels, Lipatov, SV]

Related work:

[Brower,Nastase,Schnitzer,Tan]

Some pieces by direct calculation

[Del Duca, Glover]

6. Open questions

Different aspects of the theory and phenomenology of the BFKL formalism

QCD at the LHC:

- Multijet events
- Forward physics
- Underlying event
- Diffractive processes
- Parton distribution functions at small x
- Parton saturation

Important on its own and as background to new physics.

Theoretical challenges:

- Unitarity corrections at high energy
- Correct degrees of freedom?
- Scattering amplitudes at strong coupling?
- Holography of saturation?

Connections to black hole physics might answer these questions.